EUROPEAN ORGANISATION FOR NUCLEAR RESEARCH

CERN/PPE/94-187
25 November 1994

Combined Preliminary Data on Z Parameters from the LEP Experiments and Constraints on the Standard Model *

The LEP Collaborations
ALEPH, DELPHI, L3, OPAL
and
The LEP Electroweak Working Group

Prepared from contributions of the LEP experiments
to the 27th International Conference on High Energy Physics,
Glasgow, Scotland, 20-27 July 1994

Abstract

The data recorded by the four LEP experiments until the end of 1993 correspond to approximately $8 \cdot 10^6$ Z decays into hadrons and charged leptons. This note presents a combination of published and preliminary electroweak results from the four LEP collaborations which were prepared for the 27th International Conference on High Energy Physics, Glasgow, Scotland, 20-27 July 1994. Averages of electroweak LEP results from the measurement of hadronic and leptonic cross sections, the leptonic forward-backward asymmetries, the τ polarisation asymmetries, the $b\overline{b}$ and $c\overline{c}$ partial widths and forward-backward asymmetries and the $q\overline{q}$ charge asymmetry are presented. The combined set of electroweak measurements is used to constrain the parameters of the Standard Model.

*The LEP Collaborations each take responsibility for the preliminary data of their own experiments.

1 Introduction

The four LEP experiments present updated parameters of the Z resonance derived from published data and preliminary results. Most of the preliminary results are contributions to the 27th International Conference on High Energy Physics, Glasgow, Scotland, 20-27 July 1994. The emphasis of this note is a description of the combination of electroweak parameters of the four LEP experiments, taking account of errors which are correlated among the different measurements. This combination is carried out by the LEP Electroweak Working Group[1]. The data consist of the hadronic and leptonic cross sections, the leptonic forward-backward asymmetries, the τ polarisation asymmetries, the $b\overline{b}$ and $c\overline{c}$ partial widths and forward-backward asymmetries and the $q\overline{q}$ charge asymmetry. Several aspects of such a combination have already been studied in References 1 and 2.

Since the previous combination of electroweak parameters [2] a significant development is the precise LEP energy scan carried out in 1993. With frequent measurements [3, 4] using the technique of resonant depolarisation it is possible to reduce the uncertainties due to LEP energies on the Z mass, m_Z, and width, Γ_Z, to ± 4 MeV and ± 3 MeV respectively. Coupled with the high statistics data recorded by the experiments, the total errors on m_Z and Γ_Z are greatly reduced. The analysis of the LEP energy measurements is still in progress and it is expected that even better precision will finally be obtained.

The installation of new luminosity monitors in most of the experiments leads to an improved measurement of the luminosity for the 1993 data. The experimental systematic error is now well below the theoretical uncertainty of 0.25% [5].

The measurements of the τ polarisation benefit from increased statistics. Recent studies of QED radiation in the hadronic decay modes of the τ show that the systematic errors on the polarisation from such effects are quite small.

The LEP experiments report improved measurements of the $b\overline{b}$ and $c\overline{c}$ partial widths and forward-backward asymmetries. In order to facilitate combination of the results, each experiment provides a set of seven quantities derived from their data, together with a breakdown of systematic errors in a standardised form. In this way it is possible to treat more rigorously errors which are correlated among the different analyses, and among the different experiments.

This paper is organised in the following manner. In section 2 the results on the Z lineshape and leptonic forward-backward asymmetries are presented, and section 3 contains the measurements of the τ polarisation. Section 4 describes the parameters associated with heavy flavour analyses. In sections 5.1 and 5.2 several LEP electroweak measurements are combined to determine the effective neutral current coupling constants and to give a value of the effective electroweak mixing angle. The number of light neutrinos is determined in section 5.3. In section 5.4 the LEP data and also data from SLD [6], from neutrino interactions [7–9] and from measurements of the mass of the W boson [10–12] and the top quark [13] are used to constrain the parameters of the Standard Model.

[1] The present members of the LEP Electroweak Working Group are: D. Abbaneo, A. Blondel, G. Borisov, I. Brock, D. Brown, V. Canale, D. Charlton, R. Clare, P. Clarke, T.S. Dai, S. Ganguli, M. Grünewald, A. Gurtu, A. Halley, J. Harton, R.W.L. Jones, S. De Jong, A. Kunin, M. Mannelli, M. Martinez, K. Mönig, G. Myatt, A. Olshevsky, A. Passeri, Ch. Paus, M. Pepe-Altarelli, P. Perret, B. Pietrzyk, P. Renton, D. Reid, M. Roney, D. Schaile, D. Schlatter, R. Tenchini, F. Teubert, P. Wells.

2 Z Lineshape and Lepton Forward-Backward Asymmetries

The results presented here are based on the data taken during the energy scans in 1990 and 1991 with centre-of-mass energies, $\sqrt{s}$, in a range $|\sqrt{s} - m_{\rm Z}| < 3$ GeV, the high statistics data collected at the Z peak in 1992, and a preliminary analysis of the high precision scan in 1993. During this scan more than 18 pb^{-1} were recorded by each experiment at two centre-of-mass energy points roughly 1.8 GeV above and below the Z mass while about 15 pb^{-1} was within 200 MeV of $m_{\rm Z}$.

The total statistics and the systematic errors of the individual LEP collaborations are given in Tables 1 and 2. Details of the individual analyses can be found in References 14–17. An important aspect of the lineshape analysis is a precise knowledge of the LEP centre-of-mass energies. The treatment of the LEP centre-of-mass energies by the four LEP experiments is based on the recommendations of the LEP Energy Group [3,4]. In order to determine the total Z width, $\Gamma_{\rm Z}$, all of the recorded data is combined, taking the energy uncertainty from the 1993 data to be uncorrelated with the energy uncertainty coming from previous years, resulting in an overall LEP energy error on $\Gamma_{\rm Z}$ of 2.7 MeV. However for the determination of the Z mass, $m_{\rm Z}$, only the 1993 data is used. This follows the recommendation of Reference 4, and is due to the correlation with previous years having not yet been fully studied.

For the averaging of results the LEP experiments provide a standard set of 9 parameters describing the information contained in hadronic and leptonic cross sections and leptonic forward-backward asymmetries [2]. These parameters are convenient for fitting and averaging since they have minimal correlations amongst themselves:

- The mass of the Z, $m_{\rm Z}$, and the total width, $\Gamma_{\rm Z}$, where the definition is based on the Breit Wigner denominator $(s - m_{\rm Z}^2 + is\Gamma_{\rm Z}/m_{\rm Z})$ [18].

- The hadronic pole cross section:
$$\sigma_{\rm h}^0 \equiv \frac{12\pi}{m_{\rm Z}^2}\frac{\Gamma_{\rm ee}\Gamma_{\rm had}}{\Gamma_{\rm Z}^2}\,.$$
Here $\Gamma_{\rm ee}$ and $\Gamma_{\rm had}$ are the partial widths of the Z for decays into electrons and hadrons.

- The ratios:
$$R_{\rm e} \equiv \Gamma_{\rm had}/\Gamma_{\rm ee} \qquad R_\mu \equiv \Gamma_{\rm had}/\Gamma_{\mu\mu} \qquad R_\tau \equiv \Gamma_{\rm had}/\Gamma_{\tau\tau}. \tag{1}$$
Here $\Gamma_{\mu\mu}$ and $\Gamma_{\tau\tau}$ are the partial widths of the Z for the decays $\rm Z \to \mu^+\mu^-$ and $\rm Z \to \tau^+\tau^-$. Even under the assumption of lepton universality a small (0.2%) difference between the values for $R_{\rm e}$ and R_μ, and the value for R_τ due to mass corrections to $\Gamma_{\tau\tau}$ is expected.

- The pole asymmetries, $A_{\rm FB}^{0,\rm e}$, $A_{\rm FB}^{0,\mu}$ and $A_{\rm FB}^{0,\tau}$ for the processes $\rm e^+e^- \to e^+e^-$, $\rm e^+e^- \to \mu^+\mu^-$ and $\rm e^+e^- \to \tau^+\tau^-$. In terms of the effective vector and axial-vector neutral current couplings of fermions, g_{Vf} and g_{Af}, the pole asymmetries are expressed as:[2]
$$A_{\rm FB}^{0,\rm f} \equiv \frac{3}{4}\mathcal{A}_{\rm e}\mathcal{A}_{\rm f} \tag{2}$$
with:
$$\mathcal{A}_{\rm f} \equiv \frac{2g_{Vf}g_{Af}}{g_{Vf}^2 + g_{Af}^2}\,. \tag{3}$$

[2] Effects coming from photon exchange, as well as real and imaginary parts of the photon vacuum polarisation are not included in the definition of $A_{\rm FB}^{0,\rm f}$, but are accounted for explicitly in the fitting formulae used by the experiments.

Note, that these parameters do not describe the properties of the Z completely, because they do not include the interference of the Z exchange with the photon exchange. For the results presented in this paper, the γZ interference terms are therefore fixed to their Standard Model values.[3]

The four sets of 9 parameters provided by the LEP experiments are presented in Table 3. The covariance matrix of these input parameters is as described in our previous paper [2]. It is constructed from the covariance matrices of the individual LEP experiments and common systematic errors. These common errors arise from the theoretical uncertainty in the luminosity normalisation affecting the hadronic pole cross section, $\Delta\sigma^0_{\rm h}/\sigma^0_{\rm h} = 0.25\%$; and from the energy calibration of LEP, giving $\Delta m_{\rm Z} =$ 4 MeV, $\Delta\Gamma_{\rm Z} = 2.7$ MeV, and $\Delta A^{0,\ell}_{\rm FB} = 0.0008$ for each lepton species ($\ell = {\rm e}, \mu, \tau$). Full correlation between $A^{0,\mu}_{\rm FB}$ and $A^{0,\tau}_{\rm FB}$ and full anti-correlation between $A^{0,{\rm e}}_{\rm FB}$ and $A^{0,\mu}_{\rm FB}$ or $A^{0,\tau}_{\rm FB}$ is used. This change of sign of the energy effect for $A^{0,{\rm e}}_{\rm FB}$ is an approximation of the effect of the t-channel interference for a typical LEP experimental acceptance for the ${\rm e^+e^-}$ final state. The combined parameter set and its correlation matrix are given in Tables 4 and 5.

If lepton universality is assumed, the set of 9 parameters given above is reduced to a set of 5 parameters. R_ℓ is defined as $R_\ell \equiv \Gamma_{\rm had}/\Gamma_{\ell\ell}$, where $\Gamma_{\ell\ell}$ refers to the partial Z width for the decay into a pair of massless charged leptons.

The data of each of the four LEP experiments are consistent with lepton universality (the χ^2/d.o.f. are $3/4, 6/4, 5/4$ and $3/4$ for ALEPH, DELPHI, L3 and OPAL, respectively). Based on this assumption Table 6 provides the five parameters $m_{\rm Z}$, $\Gamma_{\rm Z}$, $\sigma^0_{\rm h}$, R_ℓ and $A^{0,\ell}_{\rm FB}$ for the individual LEP experiments. The four experiments all use the above definition of $\Gamma_{\ell\ell}$. Tables 7 and 8 provide the five parameters $m_{\rm Z}$, $\Gamma_{\rm Z}$, $\sigma^0_{\rm h}$, R_ℓ and $A^{0,\ell}_{\rm FB}$ and the corresponding correlation matrix for the combined result of the 4 LEP experiments. For completeness, in Table 9 the partial decay widths of the Z boson are listed.

Figure 1 shows, for each lepton species and for the combination assuming lepton universality, the resulting 68% probability contours in the R_ℓ-$A^{0,\ell}_{\rm FB}$ plane, together with the Standard Model prediction. The χ^2/d.o.f. of the weighted average of the leptonic pole asymmetries $A^{0,{\rm e}}_{\rm FB}$, $A^{0,\mu}_{\rm FB}$ and $A^{0,\tau}_{\rm FB}$ has a value of 7.1/2. Note however, that the hypothesis of a deviation between $A^{0,\tau}_{\rm FB}$ and the average of $A^{0,{\rm e}}_{\rm FB}$ and $A^{0,\mu}_{\rm FB}$ is not supported by the τ polarisation results (see Sections 3 and 5.1).

[3] If instead the γZ interference terms are determined from LEP data, there is an additional uncertainty on $m_{\rm Z}$ of 8 MeV for a single LEP experiment.

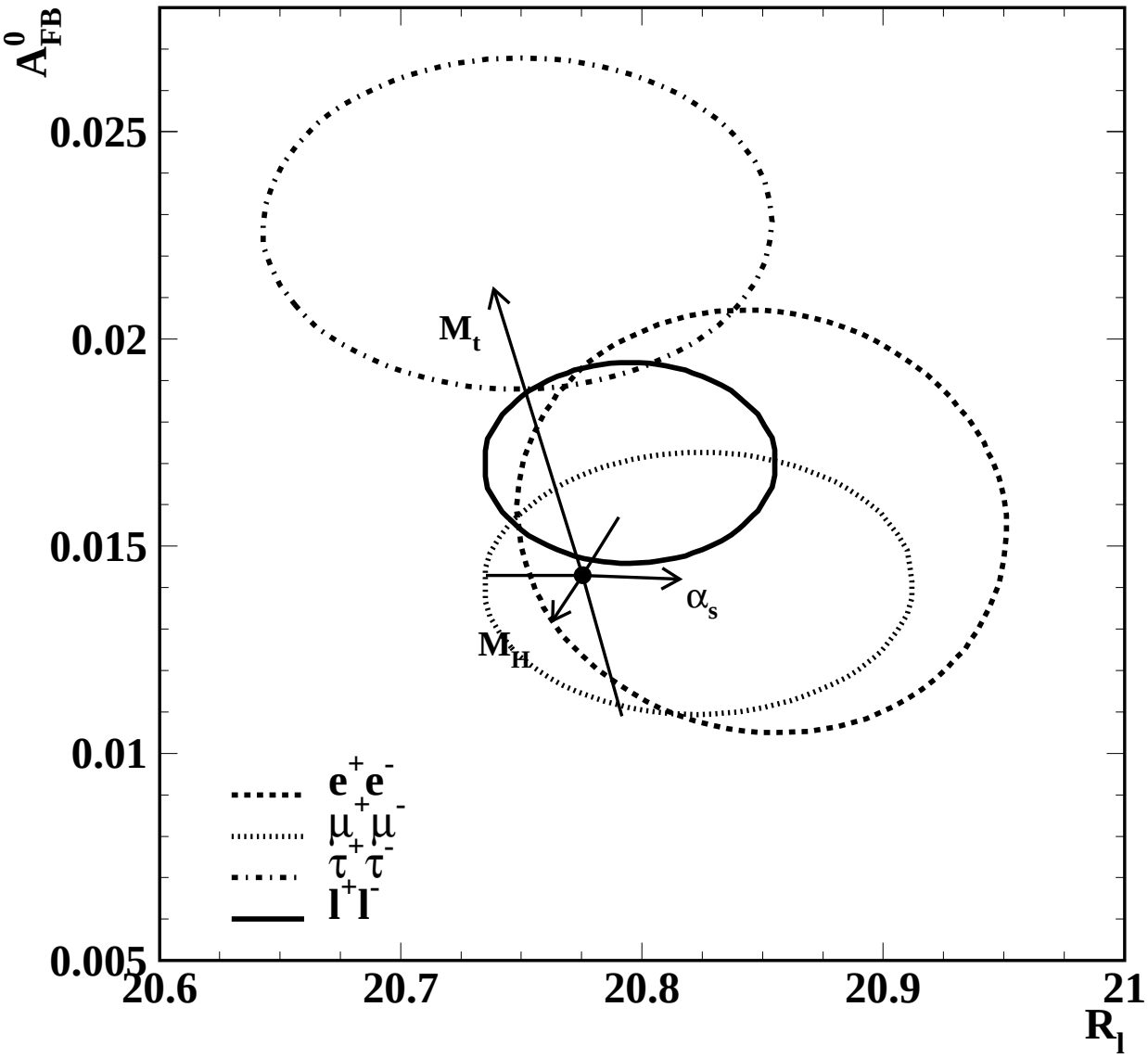

Figure 1: 68% probability contours in the R_ℓ-$A_{\rm FB}^{0,\ell}$ plane. Also shown is the Standard Model prediction for $m_{\rm Z}$ = 91.1888 GeV, $m_{\rm t}$ = 150 GeV, $m_{\rm H}$ = 300 GeV, and α_s = 0.123. The lines with arrows correspond to the variation of the Standard Model prediction when $m_{\rm t}$, $m_{\rm H}$ or α_s are varied in the intervals $50 < m_{\rm t}({\rm GeV}) < 250$, $60 < m_{\rm H}({\rm GeV}) < 1000$ and $\alpha_s(m_{\rm Z}^2) = 0.123 \pm 0.006$, respectively. The arrows point in the direction of increasing values for $m_{\rm t}$, $m_{\rm H}$ and α_s.

		ALEPH	DELPHI	L3	OPAL	LEP
$q\bar{q}$	'90-'91	451	356	416	454	1677
	'92	680	697	678	733	2788
	'93 prel.	653	677	658	653	2641
	total	1784	1730	1752	1840	7106
$\ell^+\ell^-$	'90-'91	55	37	40	58	190
	'92	82	69	58	88	297
	'93 prel.	79	71	62	81	293
	total	216	177	160	227	780

Table 1: The LEP statistics in units of 10^3 events used for the analysis of the Z line shape and lepton forward-backward asymmetries.

	ALEPH		DELPHI		L3		OPAL	
	'92	'93 prel.	'92	'93 prel.	'92	'93 prel.	'92	'93 prel.
$\mathcal{L}^{\text{exp. }(a)}$	0.15%	0.09%	0.38%	0.28%	0.5 %	0.16%	0.41%	0.07%
σ_{had}	0.14%	0.14%	0.13%	0.13%	0.15%	$0.11-0.14\%^{(b)}$	0.20%	0.20%
σ_{e}	0.4 %	0.4 %	0.59%	1.2 %	0.3 %	$0.25-0.76\%^{(b)}$	0.22%	0.23%
σ_{μ}	0.5 %	0.5 %	0.37%	0.5 %	0.5 %	$0.45-0.57\%^{(b)}$	0.19%	0.22%
σ_{τ}	0.3 %	0.3 %	0.63%	0.8 %	0.7 %	0.54%	0.44%	0.46%
$A_{\text{FB e}}$	0.003	0.003	0.003	0.003	0.002	0.005	0.002	0.002
$A_{\text{FB }\mu}$	0.001	0.001	0.001	0.002	0.002	0.001	0.001	0.001
$A_{\text{FB }\tau}$	0.0005	0.0005	0.0017	0.002	0.003	0.004	0.002	0.002

Table 2: The experimental systematic errors for the analysis of the Z line shape and lepton forward-backward asymmetries. The errors quoted do not include the common uncertainty due to the LEP energy calibration. The treatment of correlations between the errors for different years is described in References 14–17.

$^{(a)}$In addition, there is a theoretical error for the calculation of the small angle Bhabha cross section of 0.25% [5] which is common to all experiments.

$^{(b)}$The indicated range for the 1993 selection expresses the variation of the systematic error as a function of energy.

	ALEPH	DELPHI	L3	OPAL
$m_{\rm Z}$(GeV)	91.1915±0.0052	91.1870±0.0052	91.1900±0.0054	91.1862±0.0054
$\Gamma_{\rm Z}$(GeV)	2.4959±0.0061	2.4951±0.0059	2.5040±0.0058	2.4945±0.0061
$\sigma^0_{\rm h}$(nb)	41.59±0.13	41.26±0.17	41.44±0.15	41.47±0.16
R_e	20.67±0.13	20.96±0.16	20.94±0.13	20.90±0.13
R_μ	20.91±0.14	20.60±0.12	20.93±0.14	20.855±0.097
R_τ	20.69±0.12	20.64±0.16	20.70±0.17	20.91±0.13
$A^{0,\,\rm e}_{\rm FB}$	0.0212±0.0054	0.0207±0.0073	0.0109±0.0081	0.0060±0.0066
$A^{0,\,\mu}_{\rm FB}$	0.0189±0.0039	0.0128±0.0037	0.0132±0.0048	0.0124±0.0035
$A^{0,\,\tau}_{\rm FB}$	0.0253±0.0043	0.0209±0.0057	0.0299±0.0073	0.0193±0.0044
χ^2/d.o.f.	172/178	154/132	111/131	$10/6^{(a)}$

Table 3: Line shape and asymmetry parameters from 9-parameter fits to the data of the four LEP experiments.
$^{(a)}$This parameter set has been obtained from a parameter transformation applied to the 15 parameters of the OPAL fit [17], which treats the γZ interference terms for leptons as additional free parameters. The extra parameters for the γZ interference terms have not been fixed in the transformation. The χ^2/d.o.f. for the 15 parameter fit to the data is 87/125.

Parameter	Average Value
$m_{\rm Z}$(GeV)	91.1888±0.0044
$\Gamma_{\rm Z}$(GeV)	2.4974±0.0038
$\sigma^0_{\rm h}$(nb)	41.49±0.12
$R_{\rm e}$	20.850±0.067
R_μ	20.824±0.059
R_τ	20.749±0.070
$A^{0,\,\rm e}_{\rm FB}$	0.0156±0.0034
$A^{0,\,\mu}_{\rm FB}$	0.0141±0.0021
$A^{0,\,\tau}_{\rm FB}$	0.0228±0.0026

Table 4: Average line shape and asymmetry parameters from the data of the four LEP experiments given in Table 3, without the assumption of lepton universality. The χ^2/d.o.f. of the average is 26.8/27.

	$m_{\rm Z}$	$\Gamma_{\rm Z}$	$\sigma^0_{\rm h}$	$R_{\rm e}$	R_μ	R_τ	$A^{0,\,\rm e}_{\rm FB}$	$A^{0,\,\mu}_{\rm FB}$	$A^{0,\,\tau}_{\rm FB}$
$m_{\rm Z}$	1.00	0.04	0.01	−0.02	−0.01	0.00	0.02	0.03	0.02
$\Gamma_{\rm Z}$	0.04	1.00	−0.11	0.00	0.01	0.00	0.01	0.00	0.00
$\sigma^0_{\rm h}$	0.01	−0.11	1.00	0.07	0.10	0.08	0.01	0.00	0.00
$R_{\rm e}$	−0.02	0.00	0.07	1.00	0.09	0.06	−0.06	0.02	0.01
R_μ	−0.01	0.01	0.10	0.09	1.00	0.07	−0.01	0.01	0.00
R_τ	0.00	0.00	0.08	0.06	0.07	1.00	0.00	0.00	0.01
$A^{0,\,\rm e}_{\rm FB}$	0.02	0.01	0.01	−0.06	−0.01	0.00	1.00	−0.08	−0.06
$A^{0,\,\mu}_{\rm FB}$	0.03	0.00	0.00	0.02	0.01	0.00	−0.08	1.00	0.12
$A^{0,\,\tau}_{\rm FB}$	0.02	0.00	0.00	0.01	0.00	0.01	−0.06	0.12	1.00

Table 5: The correlation matrix for the set of parameters given in Table 4.

	ALEPH	DELPHI	L3	OPAL
$m_{\rm Z}$(GeV)	91.1915±0.0052	91.1869±0.0052	91.1900±0.0054	91.1862±0.0054
$\Gamma_{\rm Z}$(GeV)	2.4959±0.0061	2.4951±0.0059	2.5040±0.0058	2.4946±0.0061
$\sigma^0_{\rm h}$(nb)	41.59±0.13	41.26±0.17	41.45±0.15	41.48±0.16
R_ℓ	20.730±0.078	20.690±0.086	20.859±0.088	20.864±0.076
$A^{0,\ell}_{\rm FB}$	0.0216±0.0026	0.0160±0.0029	0.0168±0.0036	0.0137±0.0025
χ^2/d.o.f.	175/182	160/136	117/135	13/10[(a)]

Table 6: Line shape and asymmetry parameters from 5-parameter fits to the data of the four LEP experiments, assuming lepton universality.
[(a)]This parameter set has been obtained from a parameter transformation to the 15 parameters of the OPAL fit, which treats the γZ interference terms for leptons as additional free parameters.

Parameter	Average Value
$m_{\rm Z}$(GeV)	91.1888±0.0044
$\Gamma_{\rm Z}$(GeV)	2.4974±0.0038
$\sigma^0_{\rm h}$(nb)	41.49±0.12
R_ℓ	20.795±0.040
$A^{0,\ell}_{\rm FB}$	0.0170±0.0016

Table 7: Average line shape and asymmetry parameters from the results of the four LEP experiments given in Table 6, assuming lepton universality. The χ^2/d.o.f. of the average is 18.4/15.

	$m_{\rm Z}$	$\Gamma_{\rm Z}$	$\sigma^0_{\rm h}$	R_ℓ	$A^{0,\ell}_{\rm FB}$
$m_{\rm Z}$	1.00	0.04	0.01	−0.01	0.04
$\Gamma_{\rm Z}$	0.04	1.00	−0.11	0.01	0.00
$\sigma^0_{\rm h}$	0.01	−0.11	1.00	0.13	0.00
R_ℓ	−0.01	0.01	0.13	1.00	0.01
$A^{0,\ell}_{\rm FB}$	0.04	0.00	0.00	0.01	1.00

Table 8: The correlation matrix for the set of parameters given in Table 7.

Without Lepton Universality:	
$\Gamma_{\rm ee}$(MeV)	83.85±0.21
$\Gamma_{\mu\mu}$(MeV)	83.95±0.30
$\Gamma_{\tau\tau}$(MeV)	84.26±0.34

With Lepton Universality:	
$\Gamma_{\ell\ell}$(MeV)	83.96±0.18
$\Gamma_{\rm had}$(MeV)	1745.9±4.0
$\Gamma_{\rm inv}$(MeV)	499.8±3.5

Table 9: Partial decay widths of the Z boson, derived from the results of the 9-parameter (Tables 4 and 5) and the 5-parameter fit (Tables 7 and 8).

3 The τ Polarisation

3.1 Introduction

The τ polarisation $\mathcal{P}_\tau$ is determined by indirect measurement of the longitudinal polarisation of τ pairs produced in Z decays. It is defined as:

$$\mathcal{P}_\tau \equiv \frac{\sigma_R - \sigma_L}{\sigma_R + \sigma_L}\,, \tag{4}$$

where σ_R and σ_L are the τ-pair cross sections for the production of a right-handed and left-handed τ^-, respectively.

Neglecting corrections (which are actually small and discussed in section 3.2) and ignoring the effects of γ exchange, the angular distribution of $\mathcal{P}_\tau$ as a function of the angle θ between the e^- and the τ^-, for $\sqrt{s} = m_{\mathrm{Z}}$ is given by:

$$\mathcal{P}_\tau(\cos\theta) = -\frac{\mathcal{A}_\tau + \mathcal{A}_{\mathrm{e}}\frac{2\cos\theta}{1+\cos^2\theta}}{1 + \mathcal{A}_\tau\mathcal{A}_{\mathrm{e}}\frac{2\cos\theta}{1+\cos^2\theta}}\,, \tag{5}$$

with $\mathcal{A}_{\mathrm{e}}$ and $\mathcal{A}_\tau$ defined in Equation (3). When averaged over all production angles $\mathcal{P}_\tau$ is a measurement of $\mathcal{A}_\tau$, while as a function of $\cos\theta$, $\mathcal{P}_\tau(\cos\theta)$ provides nearly independent determinations of both $\mathcal{A}_\tau$ and $\mathcal{A}_{\mathrm{e}}$, allowing thus a test of the universality of the couplings of the Z to e and τ.

Each experiment makes separate $\mathcal{P}_\tau$ measurements using the five τ decay modes $e\nu\overline{\nu}$, $\mu\nu\overline{\nu}$, $\pi\nu$, $\rho\nu$ and $a_1\nu$ [19–21]. The $\rho\nu$ and $\pi\nu$ are the most sensitive channels, contributing weights of about 40% each in the average. In addition, DELPHI have used an inclusive hadronic analysis. The combination is made on the results from each experiment already averaged over the τ decay modes measured by the experiment.

3.2 Possible Common Systematic Errors

There are systematic effects in the measurements which are common to the four experiments. These are divided into two classes. The first class affects all decay modes in the same way. In general these have been studied carefully and the uncertainties in the corrections applied are small. The second class covers effects which are different for each τ decay mode. In general these are not as well studied and may be more serious than the first class of systematics.

In order to extract $\mathcal{A}_\tau$ and $\mathcal{A}_{\mathrm{e}}$ from the measured values of $\mathcal{P}_\tau$ and its variation as a function of polar-angle, the following effects are taken into account. These affect all τ decay modes equally:

- $\sqrt{s}$ dependence and the effects of γ and γZ interference. The results are corrected to correspond to $\mathcal{P}_\tau(\sqrt{s} = m_{\mathrm{Z}})$.
- Electromagnetic radiative corrections for initial state radiation from the e^+ and e^- and final state radiation from the τ^+ and τ^-.
- Mass terms leading to helicity flip configurations.

These three effects are theoretically well defined and are calculated to adequate precision for present needs [22–24]. Their combined effect is to reduce the strength of the measured polarisation by a

small amount. The experiments correct for this by computing the size of the correction, which in practice amounts to adding about 0.003 to the measured values of $\mathcal{A}_\tau$ and $\mathcal{A}_e$. The uncertainty in this correction is estimated to be less than ± 0.001.

The V$-$A theory for the τ decay is normally assumed implicitly in the experimental analysis. Of course, this theory, which is part of the Standard Model, has been tested to good accuracy in μ decays. However, if the V$-$A theory in τ decay is not imposed in the analysis, then the extracted precision of $\mathcal{P}_\tau$ is much reduced. Analyses of the V$-$A structure of τ decays have been carried out by the ALEPH [25] and ARGUS [26] Collaborations. They show that if the V$-$A assumption in τ decays is dropped the additional uncertainty which should be included in the average τ polarisation is about ± 0.005. In this analysis V$-$A is assumed with no associated error.

Since the τ polarisation is not measured directly, properties of the particular τ decay modes enter into the measurement. This introduces new theoretical uncertainties, in particular from the radiative corrections and model dependencies for the hadronic τ decays. A survey of the systematic errors given by the four experiments for the decay modes analysed shows that two common systematic errors should be considered when combining the results. Other sources of systematic errors examined remain negligible. The two common errors are:

- Model dependence of the a_1 decay: Model dependent uncertainties in a_1 decay have been evaluated to give an estimated systematic error in $\mathcal{P}_\tau$ of ± 0.012 for ALEPH and ± 0.015 for DELPHI. For all experiments there is some influence of the uncertainty on the a_1 on the results in the ρ channel. Although the meaning of the theory error differs somewhat from experiment to experiment, in principle this error should be taken to be fully correlated between experiments. A more detailed investigation of this error in the future is desirable and this would probably reduce the common error.

  In practice the a_1 decay mode does not carry a large weight in the average polarisation. The "theory error" induces an uncertainty ± 0.001 on the final polarisation value (i.e. after combining the decay channels). This is negligible at the present level of precision. The same applies for the effect on the forward-backward polarisation asymmetry.

- Radiative corrections for τ hadronic final states: Unlike radiation from leptons, there is no precise formalism for handling these corrections. However, results of recent theoretical work [27,28] on the understanding of the precision of the decay radiation model as implemented in PHOTOS [23] have become available. These suggest that the possible systematic error on the size of the radiative correction for the $\tau \to \pi\nu$ mode is at the 5% level. Consequently, the uncertainties in the decay radiation treatment contribute much less than 0.001 to the overall systematic error. For the $\tau \to \rho\gamma\nu$ decay, however, no analogous theoretical studies have yet been performed and the correction is assumed to have a systematic error of the order of $1/\ln(m_\tau/m_\rho) \approx 1.3$ of the correction itself. Recent studies indicate that these lead to a systematic error of no more than 0.001 on $\mathcal{A}_\tau$ and a negligible error on $\mathcal{A}_e$.

3.3 Results

Tables 10 and 11 show the most recent, and still mostly preliminary, results for $\mathcal{A}_\tau$ and $\mathcal{A}_e$ obtained by the four experiments [19–21][4] and their combination. No common systematics are included in these averages. The statistical correlation between the extracted values of $\mathcal{A}_\tau$ and $\mathcal{A}_e$ is small ($\leq 4\%$) and neglected.

[4]Since the Glasgow Conference, the L3 collaboration has finalized their analysis with reduced systematic errors [29], which is not included in the results presented here.

The average values for $\mathcal{A}_\tau$ and $\mathcal{A}_e$:

$$\mathcal{A}_\tau = 0.143 \pm 0.010\,, \tag{6}$$

$$\mathcal{A}_e = 0.135 \pm 0.011\,, \tag{7}$$

are compatible, as is expected from lepton universality. Assuming lepton universality, the values for $\mathcal{A}_\tau$ and $\mathcal{A}_e$ can be combined. This combination is performed neglecting any possible common systematic error between $\mathcal{A}_\tau$ and $\mathcal{A}_e$ within a given experiment. Such errors are estimated to be small, but warrant further study. The combined result of $\mathcal{A}_\tau$ and $\mathcal{A}_e$ gives:

$$\mathcal{A}_\ell = 0.139 \pm 0.007\,. \tag{8}$$

For the future, further study of the uncertainties from the effects of radiative corrections for the ρ decay-mode of the τ is desirable.

ALEPH	('90 - '92), prel.	$0.137 \pm 0.012 \pm 0.008$
DELPHI	('90 - '92), prel.	$0.144 \pm 0.018 \pm 0.016$
L3	('90 - '93), prel.	$0.144 \pm 0.013 \pm 0.015$
OPAL	('90 - '92), final	$0.153 \pm 0.019 \pm 0.013$
LEP Average		0.143 ± 0.010

Table 10: LEP results for $\mathcal{A}_\tau$. The χ^2/d.o.f. for the average is 0.4/3

ALEPH	('90 - '92), prel.	$0.127 \pm 0.016 \pm 0.005$
DELPHI	('90 - '92), prel.	$0.140 \pm 0.028 \pm 0.003$
L3	('90 - '93), prel.	$0.154 \pm 0.020 \pm 0.012$
OPAL	('90 - '92), final	$0.122 \pm 0.030 \pm 0.012$
LEP Average		0.135 ± 0.011

Table 11: LEP results for $\mathcal{A}_e$. The χ^2/d.o.f. for the average is 1.1/3

4 Electroweak Results with b and c Quarks

4.1 Introduction

For the purpose of averaging electroweak results in the heavy flavour sector, the LEP experiments provide a standard set of seven quantities which describe:

- The ratios of the b and c quark partial widths to the total hadronic partial width: $R_{\mathrm{b}} \equiv \Gamma_{\mathrm{b\bar{b}}}/\Gamma_{\mathrm{had}}$ and $R_{\mathrm{c}} \equiv \Gamma_{\mathrm{c\bar{c}}}/\Gamma_{\mathrm{had}}$.
- The forward-backward asymmetries, $A_{\mathrm{FB}}^{\mathrm{b\bar{b}}}$ and $A_{\mathrm{FB}}^{\mathrm{c\bar{c}}}$, determined at three centre-of-mass energies: on-peak, above peak and below peak.
- The semileptonic branching ratios, BR($\mathrm{b} \to \ell$) and BR($\mathrm{b} \to \mathrm{c} \to \ell^+$), and the average $\mathrm{B}^0\overline{\mathrm{B}^0}$ mixing parameter, $\overline{\chi}$. These are determined from multiparameter fits to lepton spectra and are important as they contribute to systematic uncertainties of other measurements.

4.2 Methods of Tagging Heavy Flavours

Tagging of heavy flavour production by identifying a lepton in the decay products is possible because of the characteristically large longitudinal and transverse lepton momenta arising from the large quark masses. In addition, the transverse lepton momentum is typically smaller for c decays than for b decays, allowing the two categories to be separated. The disadvantage of the lepton tag is the small semileptonic branching ratio for b and c quarks, of about 10% for e and for μ separately, compounded with lepton identification inefficiencies. This leads to b quark tagging efficiencies of about 10% for 90% purities [30–34]. The fitted quantities from lepton analyses are strongly correlated, and common systematic uncertainties lead to correlations between the results from the different experiments. It is therefore useful to average the results of these fits as a group, rather than including them as individual measurements from each experiment. The dominant common systematic errors for R_{b}, R_{c} and $A_{\mathrm{FB}}^{\mathrm{c\bar{c}}}$ are the semileptonic branching ratios, especially BR($\mathrm{b} \to \mathrm{c} \to \ell^+$) and BR($\mathrm{c} \to \ell$), and the semileptonic decay models. The systematic errors for $A_{\mathrm{FB}}^{\mathrm{b\bar{b}}}$ are significantly smaller than the statistical error so that the average is still dominated by statistics. Event shape variables, again taking advantage of the large b-quark mass, have also been used to tag $\mathrm{b\overline{b}}$ events [35,36]. A new and powerful tagging technique, in particular for the measurement of the b partial width, exploits the decay lengths of a few millimeters of b hadrons, which can easily be resolved with microvertex detectors. The hemisphere tagging efficiencies achieved for b quarks are of the order of 25% for 95% purity [33,37,38], when the event has been divided into two hemispheres by a plane perpendicular to the thrust axis.

R_{b} is currently best measured by analyses that compare the number of events with only one hemisphere tagged with that of events with both hemispheres tagged ("double-tagging methods"). This can be performed using either lifetime tags, event shapes or leptons to select the hemispheres. These methods allow the b-tagging efficiency to be derived directly from the data. Results including a lifetime tag dominate the measurements of R_{b} [33,37–39]. The dominant common systematic errors in these analyses are from the uncertainties in the charm meson lifetimes, decay multiplicities and relative fractions, and the correlations between the two hemispheres. By way of illustration, a full breakdown of the errors is given in Table 12 for the five measurements of R_{b} which are not derived from multiparameter lepton fits.

Measurements of $A_{\mathrm{FB}}^{\mathrm{b\bar{b}}}$ based on lifetime tagged events with a hemisphere charge measurement are also available. ALEPH and OPAL have determined the mean b-hemisphere charge from the charge

	ALEPH shape [35]	ALEPH lifetime [37]	DELPHI multiple [33]	L3 shape [36]	OPAL multiple [38]
Charm production	0.0	-0.85	-1.40	0.0	-0.89
D^0 lifetime	0.0	-0.28	-0.20	0.0	-0.22
D^+ lifetime	0.0	-0.36	-0.30	0.0	-0.28
D_s lifetime	0.0	-0.22	-0.20	0.0	-0.17
D decay multip.	0.0	-0.57	-0.50	0.0	-0.73
BR(D$\rightarrow$K^0)	0.0	0.0	$+0.70$	0.0	$+0.57$
$g \rightarrow b\overline{b}, c\overline{c}$	0.0	-0.33	-0.22	0.0	-0.48
Long-lived light hadrons	0.0	-0.24	-0.70	0.0	-0.49
BR($c \rightarrow \ell$)	$+0.6$	0.0	-0.30	0.0	-0.28
Semilept.mod. $c \rightarrow \ell$	-2.1	0.0	-0.20	0.0	-0.24
$\langle x_E(c) \rangle$	$+0.8$	-0.12	-0.40	$+1.8$	-0.72
Semilept model $b \rightarrow \ell$	-1.3	0.0	0.0	0.0	0.0
$\langle x_E(b) \rangle$	0.0	0.0	0.0	-3.1	0.0
Total corr. error	2.7	1.2	1.9	3.6	1.8

Table 12: Example of breakdown of the correlated systematic error for R_b from lifetime, multiple and shape double-tag measurements (in units of 10^{-3}). The sign is the sign of the correlation among the experiments.

distributions themselves [40, 41], while DELPHI makes use of lepton information in the opposite hemisphere [34]. The dominant systematic error is the light quark fragmentation.

Neither lepton tagging nor lifetime tagging allows a clean sample of charm events to be isolated. However, while both b and c events may give rise to $D^{*\pm}$ mesons, selecting $D^{*\pm}$ mesons which carry a large fraction of the beam energy allows a relatively pure charm sample to be obtained [42, 43]. Lifetime, lepton and event shape information may also be used to separate the b and c sources [44–46].

Except for the measurements of forward-backward asymmetries, the other heavy flavour electroweak measurements have systematic errors roughly as large as those from statistics. Thus the combination of different measurements requires a careful assessment of common systematic errors.

4.3 Summary of Measurements

Measurements of the seven heavy flavour quantities are provided in the form of standard tables [47–49] by the four LEP collaborations. The tables include a detailed breakdown of the systematic error of each measurement and its dependence on other electroweak parameters. Where necessary, the experiments apply **small corrections to the results quoted in their papers and notes** in order to use agreed values and ranges for the input parameters used to calculate systematic errors. These results, corrected where necessary, are summarised in the Appendix in Tables 20-29, where the statistical and systematic errors are quoted separately. The correlated systematic entries are from sources shared with one or more other results in the table and are derived from the full breakdown of common systematic uncertainties. The uncorrelated systematic entries are from the remaining sources.

The results in References 50–53, which were used in previous heavy flavour averages, are no longer included. Some are superseded by the results presented here, while the rest are not sufficiently precise to affect the averages, or to merit the detailed study of systematic errors which is now required, and are removed to simplify the averaging procedure.

Since c-quark events form the main background in the R_b analyses, the value of R_b depends on the value of R_c. If R_b and R_c are measured in the same analysis, this is reflected in the correlation matrix for the results. Otherwise, this dependence may be written as:

$$R_b = R_b^{meas} + a_c \frac{(R_c - R_c^{used})}{R_c}. \quad (9)$$

In this expression, R_b^{meas} is the result of the analysis which assumed a value of $R_c = R_c^{used}$. The values of R_c^{used} and the coefficients a_c are given in Table 20 where appropriate. The dependences of all other measurements on other electroweak parameters are treated in the same way.

Forward-backward asymmetries are translated to the following centre-of-mass energies:

$$\begin{aligned} \sqrt{s} &= 89.55 \text{ GeV } (\text{“}-2\text{”}), \\ \sqrt{s} &= 91.26 \text{ GeV } (\text{“pk”}) , \\ \sqrt{s} &= 92.94 \text{ GeV } (\text{“}+2\text{”}). \end{aligned}$$

These were chosen so as to be close to the $\sqrt{s}$ values at which measurements were made so that the corrections are generally small. The predicted Standard Model $\sqrt{s}$ dependence from ZFITTER was used. After calculating the overall averages, the corrections described in section 4.4 were made to the average peak asymmetries to derive the pole asymmetries.

4.4 Corrections to asymmetries

In general, the measured asymmetries assume that the differential cross section has the form:

$$\frac{d\sigma}{d\cos\theta} \propto 1 + \cos^2\theta + \frac{8}{3} A_{FB} \cos\theta, \quad (10)$$

where θ is the angle between the direction of the incoming electron and outgoing quark. The event thrust axis is used as an estimate of the quark direction. Small corrections are then applied to relate the measured asymmetries to the pole asymmetries. Only the asymmetries measured at the peak ($\sqrt{s} = 91.26$ GeV) have been used to determine the pole asymmetries. The corrections are summarised in Table 13 and explained below:

- Energy shift correction: The slope of the asymmetry as a function of $\sqrt{s}$ around m_Z depends only on the axial coupling and the charge of the initial and final state fermions and is thus independent of the pole asymmetry itself.
- QED corrections: Initial state radiation reduces the effective centre-of-mass energy. Thus a correction similar in nature to the energy shift must be applied.
- QCD corrections: The QCD corrections using the thrust axis as the event axis have been calculated recently by Lampe [54] and are of the form $A_{FB}^{QCD} = A_{FB}^{no\,QCD}(1 + c\frac{\alpha_s}{\pi})$, where $c = -0.893$ for massless quarks. The mass effects for b and c quarks have been calculated for the case where the quark direction is taken as the event axis [55]. These mass corrections have been assumed to be valid for the thrust axis calculation. An additional uncertainty of 25% of the overall QCD correction is assigned to account for this assumption, and for the question of bias in the thrust axis distribution introduced by experimental event selection cuts.

  Although the measured asymmetries using a lepton or $D^\star$ meson tag need to be corrected in this way for the effects of QCD, the lifetime/hemisphere-charge measurements of the b asymmetry take into account QCD effects as an inherent part of the analysis [34,40,41]. To form a consistent average, the QCD correction for the b asymmetry of $+0.0027$ is therefore subtracted from each of these hemisphere charge measurements before combining with the other measurements.

- γ exchange and γZ interference: These diagrams modify very slightly the asymmetry.

All corrections with the exception of the QCD corrections have been determined using ZFITTER [24].

Source	$\delta A_{\rm FB}^{\rm b\bar{b}}$	$\delta A_{\rm FB}^{\rm c\bar{c}}$
$\sqrt{s} = m_{\rm Z}$	–0.0013	–0.0034
QED corrections	+0.0041	+0.0104
QCD corrections	$+0.0027 \pm 0.0010$	$+0.0022 \pm 0.0005$
γ, γZ	–0.0003	–0.0008
Total	$+0.0052 \pm 0.0010$	$+0.0084 \pm 0.0005$

Table 13: Corrections to be applied to the quark asymmetries. The corrections are to be understood as $A_{\rm FB}^0 = A_{\rm FB}^{meas} + \sum_i (\delta A_{\rm FB})_i$

4.5 Averaging Procedure and Results

The averaging procedure used was a χ^2 minimisation for all the electroweak parameters listed in section 4.1. The explicit dependences of each measurement on the other electroweak parameters was taken into account, for example the dependence of the value of $R_{\rm b}$ on the assumed value of $R_{\rm c}$ described in equation 9. The full statistical and systematic covariance matrix for all the measurements was calculated. The correlation matrices relating several measurements made in the same analyses were used, in particular for the multiparameter lepton fits. The correlations among the measurements from different analyses or by different LEP experiments, which arise from common sources of systematic uncertainty, were estimated from a detailed breakdown of systematic errors [47]. This breakdown for the double-tag measurements of $R_{\rm b}$, plus the L3 event shape analysis which also measures this single parameter, is given in Table 12.

Several cross checks were made in order to ensure that the combined estimate is reliable. For example, a weighted average for each parameter, taking into account the common systematic errors given in Tables 20-29, was formed. The smallest common systematic error was assumed to be fully correlated. This is justifiable as the common systematic errors are often less than half of the statistical error. Differences between the results of the full procedure and the simpler weighted averages are small, typically less than 20% of the error, thus giving confidence in the more complete procedure. As an example, results for $R_{\rm b}$ are compared in Table 14. In this table, the averages of the five single-parameter analyses, dominated by the double-tag measurements, are compared in the first column, $R_{\rm b}$ measurements from the multiparameter lepton fits in the second column, and all measurements of $R_{\rm b}$ in the third column. These comparisons are all made with the value of $R_{\rm c}$ fixed to 0.171.

Using the full averaging procedure gives the following combined results for the electroweak param-

	$R_{\rm b}$ single param.	$R_{\rm b}$ lepton fits	$R_{\rm b}$ combined
Average	0.2195 ± 0.0021	0.2178 ± 0.0055	0.2193 ± 0.0019
Full Fit	0.2197 ± 0.0020	0.2173 ± 0.0048	0.2192 ± 0.0018

Table 14: Comparison of $R_{\rm b}$ between weighted average and full fit for $R_{\rm c}$=0.171.

	R_c	BR($b \to \ell$)	BR($bc\ell$)	$\overline{\chi}$	$A_{FB}^{b\bar{b}}$(pk)	$A_{FB}^{c\bar{c}}$(pk)
R_b	−0.38	−0.33	0.02	−0.06	−0.03	0.08
R_c		0.28	−0.09	−0.12	0.10	−0.07
BR($b \to \ell$)			0.08	0.19	0.04	0.05
BR($bc\ell$)				−0.84	−0.13	−0.21
$\overline{\chi}$					0.18	0.05
$A_{FB}^{b\bar{b}}$(pk)						0.12

Table 15: Correlation matrix of the final result. The correlations between the off-peak asymmetries and the other measurements are small (less than 0.1) and have been omitted. (BR($bc\ell$) $\equiv$ BR($b \to c \to \ell^+$)).

eters:

$$\begin{aligned} R_b &= 0.2202 \pm 0.0020 \\ R_c &= 0.1583 \pm 0.0098 \\ A_{FB}^{b\bar{b}}(-2) &= 0.044 \pm 0.015 \\ A_{FB}^{c\bar{c}}(-2) &= -0.181 \pm 0.039 \\ A_{FB}^{b\bar{b}}(\text{pk}) &= 0.0915 \pm 0.0037 \\ A_{FB}^{c\bar{c}}(\text{pk}) &= 0.0675 \pm 0.0091 \\ A_{FB}^{b\bar{b}}(+2) &= 0.105 \pm 0.013 \\ A_{FB}^{c\bar{c}}(+2) &= 0.095 \pm 0.035 \end{aligned}$$

In addition, the combined values for the semileptonic branching ratios and the mixing parameter are: BR($b \to \ell$) $= 0.1099 \pm 0.0025$, BR($b \to c \to \ell^+$) $= 0.0807 \pm 0.0044$, and $\overline{\chi} = 0.1149 \pm 0.0069$. The overall χ^2/d.o.f. is $34.3/(58-11)$, and the correlation matrix is given in Table 15. One problem was revealed by the cross checks: the error on the average value of BR($b \to \ell$) was found to be sensitive to the fitting procedure. The error on this measurement is dominated by the uncertainties in the semileptonic decay model. The relative sign of this error is not the same for all the analyses, which leads to cancellations in the averaging procedure. This requires further study before the error on BR($b \to \ell$) can be considered reliable. Changing the assumptions on the treatment of BR($b \to \ell$) suggests that an overall error of about 0.004 would be reasonable. It should be stressed that the central value for BR($b \to \ell$), and the values and errors for the other electroweak parameters, were found to be extremely robust to these changes. The exact values of the correlations between BR($b \to \ell$) and the other parameters depend on the error on BR($b \to \ell$).

The main electroweak results can be summarised using the pole asymmetries $A_{FB}^{0,b}$ and $A_{FB}^{0,c}$, as defined by equations 2 and 3:

$$\begin{aligned} R_b &= 0.2202 \pm 0.0020 \\ R_c &= 0.1583 \pm 0.0098 \\ A_{FB}^{0,b} &= 0.0967 \pm 0.0038 \\ A_{FB}^{0,c} &= 0.0760 \pm 0.0091 \end{aligned}$$

with correlations between the results as given in Table 15. The value of R_b with R_c fixed to its expected Standard Model value is:

$$R_b(R_c = 0.171) = 0.2192 \pm 0.0018.$$

5 Interpretation of Results

5.1 The Effective Z Couplings

The partial widths of the Z into leptons and the lepton forward-backward asymmetries (Section 2), the τ polarisation and the τ polarisation asymmetry (Section 3) can all be combined to determine the effective vector and axial vector couplings for e, μ and τ. The asymmetries (Equations 2 and 5) determine the ratio $g_{V\ell}/g_{A\ell}$ (Equation 3), while the sum of the squares of the couplings is derived from the leptonic partial widths:

$$\Gamma_{\ell\ell} = \frac{G_{\rm F} m_{\rm Z}^3}{6\pi\sqrt{2}}(g_{V\ell}^2 + g_{A\ell}^2)(1+\delta_\ell^{QED}) \,, \tag{11}$$

where $\delta_\ell^{QED} = 3q_\ell^2\alpha(m_{\rm Z}^2)/(4\pi)$ accounts for final state photonic corrections.

The averaged results for the effective lepton couplings are given in Table 16. Figure 2 shows the 68% probability contours in the $g_{A\ell}$-$g_{V\ell}$ plane. The signs of $g_{A\ell}$ and $g_{V\ell}$ are based on the convention $g_{A{\rm e}} < 0$. With this convention the signs of the couplings of all charged leptons follow from LEP data alone. The measured ratios of the e, μ and τ couplings provide a test of lepton universality:

$$\begin{aligned} g_{V\mu}/g_{V{\rm e}} &= 0.83 \ \pm 0.16 \ , \ g_{A\mu}/g_{A{\rm e}} = 1.0014 \pm 0.0021, \\ g_{V\tau}/g_{V{\rm e}} &= 1.044 \pm 0.091, \ g_{A\tau}/g_{A{\rm e}} = 1.0034 \pm 0.0023. \end{aligned}$$

The neutrino coupling can be derived from the measured value of the invisible width of the Z, $\Gamma_{\rm inv}$, attributing it exclusively to the decay into three identical neutrino generations ($\Gamma_{\rm inv} = 3\Gamma_{\nu\nu}$) and assuming $g_{A\nu} = g_{V\nu} \equiv g_\nu$. The sign of g_ν is chosen to be in agreement with neutrino scattering data [56], resulting in

$$g_\nu = +0.5011 \pm 0.0018.$$

Without Lepton Universality:	
$g_{V{\rm e}}$	-0.0370 ± 0.0021
$g_{V\mu}$	-0.0308 ± 0.0051
$g_{V\tau}$	-0.0386 ± 0.0023
$g_{A{\rm e}}$	-0.50093 ± 0.00064
$g_{A\mu}$	-0.50164 ± 0.00096
$g_{A\tau}$	-0.5026 ± 0.0010

With Lepton Universality:	
$g_{V\ell}$	-0.0366 ± 0.0013
$g_{A\ell}$	-0.50128 ± 0.00054
g_ν	$+0.5011 \pm 0.0018$

Table 16: Results for the effective vector and axial vector couplings derived from the combined LEP data without and with the assumption of lepton universality.

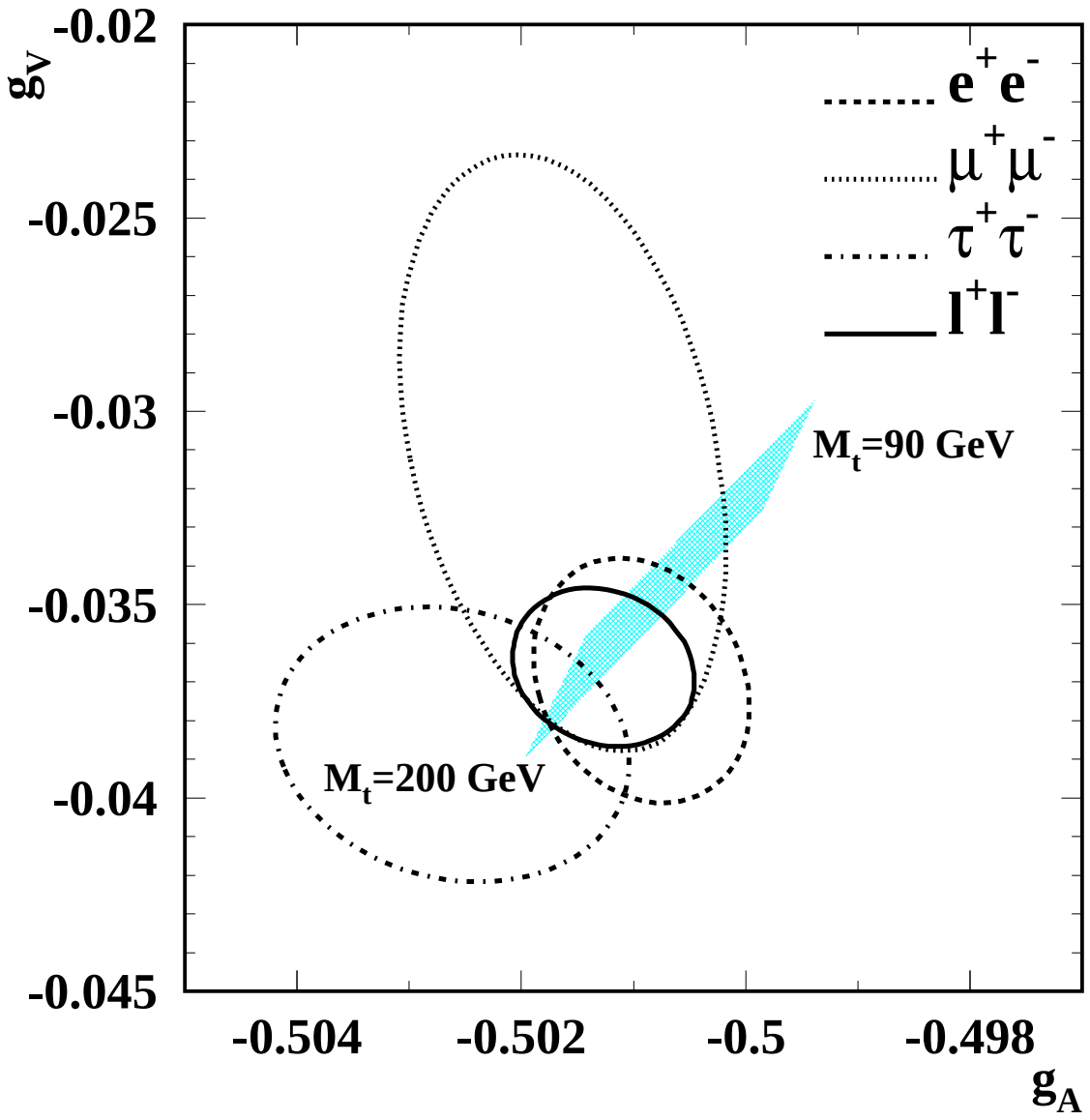

Figure 2: The 68% probability contours in the $g_{V\ell}$-$g_{A\ell}$ plane. The solid contour results from a fit assuming lepton universality. The shaded band represents the Standard Model prediction.

5.2 The Effective Electroweak Mixing Angle $\sin^2\theta^{\rm lept}_{\rm eff}$

The asymmetry measurements from LEP can be combined into a single observable, the effective electroweak mixing angle, $\sin^2\theta^{\rm lept}_{\rm eff}$, defined as:

$$\sin^2\theta^{\rm lept}_{\rm eff} \equiv \frac{1}{4}(1 - g_{V\ell}/g_{A\ell})\,, \tag{12}$$

without making any strong model-specific assumptions.

For a combined average of $\sin^2\theta^{\rm lept}_{\rm eff}$ from $A^{0,\ell}_{\rm FB}$, $\mathcal{A}_\tau$ and $\mathcal{A}_{\rm e}$ only the assumption of lepton universality, already inherent in the definition of $\sin^2\theta^{\rm lept}_{\rm eff}$, is needed. In practice no further assumption is involved if the quark forward-backward asymmetries, $A^{\rm b\bar{b}}_{\rm FB}$ and $A^{\rm c\bar{c}}_{\rm FB}$, are included in this average, as these asymmetries have a reduced sensitivity to corrections particular to the hadronic vertex. The results of these determinations of $\sin^2\theta^{\rm lept}_{\rm eff}$ and their combination are shown in Table 17. Also the comparison with the measurement of the left-right asymmetry, $A_{\rm LR}$, at SLD [6] is given. It should be noted that $A_{\rm LR}$ measures the same quantity as $\mathcal{A}_{\rm e}$ from τ polarisation, with minimal model dependence.

	$\sin^2\theta^{\rm lept}_{\rm eff}$	Average by Group of Observations	Cumulative Average	χ^2/d.o.f.
$A^{0,\ell}_{\rm FB}$	0.2311 ± 0.0009			
$\mathcal{A}_\tau$	0.2320 ± 0.0013			
$\mathcal{A}_{\rm e}$	0.2330 ± 0.0014	0.2317 ± 0.0007	0.2317 ± 0.0007	1.4/2
$A^{0,\rm b}_{\rm FB}$	0.2327 ± 0.0007			
$A^{0,\rm c}_{\rm FB}$	0.2310 ± 0.0021	0.2325 ± 0.0006	0.2321 ± 0.0005	2.8/4
$\langle Q_{\rm FB}\rangle^{(a)}$	0.2320 ± 0.0016	0.2320 ± 0.0016	0.2321 ± 0.0004	2.8/5
$A_{\rm LR}$ (SLD)	0.2294 ± 0.0010	0.2294 ± 0.0010	0.2317 ± 0.0004	9.0/6

Table 17: Comparison of several determinations of $\sin^2\theta^{\rm lept}_{\rm eff}$ from asymmetries. Averages are obtained as weighted averages assuming no correlations. The second column lists the $\sin^2\theta^{\rm lept}_{\rm eff}$ values derived from the quantities listed in the first column. The third column contains the averages of these numbers by groups of observations, where the groups are indicated by the horizontal lines. The last column shows the cumulative averages. The χ^2 per degree of freedom for the cumulative averages also is given. $^{(a)}$The status of LEP results related to the hadronic charge asymmetry [57–60], $\langle Q_{\rm FB}\rangle$, and their method of combination is unchanged with respect to Reference 2.

5.3 Number of Neutrinos

An important aspect of our measurement concerns the information related to Z decays into invisible channels. Using the results of Tables 7 and 8 the ratio of the Z decay width into invisible particles and the leptonic decay width is determined:

$$\Gamma_{\rm inv}/\Gamma_{\ell\ell} \;=\; 5.953 \pm 0.046\,.$$

Dividing this by the Standard Model value for the ratio of the partial widths to neutrinos and charged leptons:

$$(\Gamma_{\nu\nu}/\Gamma_{\ell\ell})_{\rm SM} \;=\; 1.992 \pm 0.003\,,$$

where the central value is evaluated for $m_{\rm Z}$ = 91.1888 GeV, $m_{\rm t}$ = 175 GeV, $m_{\rm H}$ = 300 GeV and the error quoted accounts for a variation of $m_{\rm t}$ in the range $100 < m_{\rm t}({\rm GeV}) < 200$ and a variation of $m_{\rm H}$ in the range $60 < m_{\rm H}({\rm GeV}) < 1000$, the number of light neutrinos is found to be:

$$N_\nu \quad = \quad 2.988 \pm 0.023.$$

5.4 Standard Model Constraints

The precise electroweak measurements performed at LEP can be used to check the validity of the Standard Model and, within its framework, to infer valuable information about its basic parameters. Their accuracy makes them sensitive to the top quark mass, $m_{\rm t}$, and to the mass of the Higgs boson, $m_{\rm H}$, through the loop corrections. The leading top quark dependence is quadratic and allows a determination of $m_{\rm t}$. The main dependence on $m_{\rm H}$ is logarithmic and therefore, with the present data accuracy, the constraints on $m_{\rm H}$ are still weak.

The various measurements are summarised in Table 18 and presented in Figure 3 and 4 together with their Standard Model prediction as a function of $m_{\rm t}$. The bands in the Standard Model predictions reflect the linear sum of the expected variations of each quantity due to a change of the strong coupling constant $\alpha_s(m_{\rm Z}^2) = 0.123 \pm 0.006$ [61] and $m_{\rm H}$ in the interval $60 \leq m_{\rm H}$ [GeV] ≤ 1000 for $m_{\rm Z}$ = 91.1888 GeV.

Table 19 shows the constraints obtained on $m_{\rm t}$ and $\alpha_s(m_{\rm Z}^2)$ when fitting the measurements in Table 18 to the most up to date Standard Model calculations [63] as verified by the working group on 'Precision Calculations at LEP-I' [64]. The fits have been repeated for $m_{\rm H}$ = 60, 300 and 1000 GeV and the difference in the fitted parameters is quoted as the second uncertainty. Presented in Table 19 are the results obtained using only LEP data (Table 18a), as well as those obtained by including the measurements of $m_{\rm W}$ from UA2 [10], CDF [11,12] and D0 [12], and the measurements of the neutrino neutral to charged current ratios from CDHS [7], CHARM [8] and CCFR [9] (Table 18b), as well those obtained by including the SLD result for the left-right asymmetry, $A_{\rm LR}$ [6] (Table 18c). The χ^2/d.o.f. for all these fits is acceptable.

The value of $\alpha_s(m_{\rm Z}^2)$ resulting from the fits of Table 19 is in very good agreement with that obtained from event shape measurements at LEP ($\alpha_s(m_{\rm Z}^2) = 0.123 \pm 0.006$ [61]) and of similar precision. The strong coupling constant can also be determined from the parameter R_ℓ alone. For $m_{\rm Z}$ = 91.1888 GeV, $m_{\rm t}$ = 175 GeV and $m_{\rm H}$ = 300 GeV, $\alpha_s = 0.126 \pm 0.006$ is obtained, where the error quoted accounts for experimental uncertainties only. A detailed discussion of theoretical uncertainties in the determination of α_s from R_ℓ can be found in Reference 65.

Similarly, the value of $m_{\rm t}$ resulting from these fits is in excellent agreement with the value recently reported by CDF [13] of $m_{\rm t} = 174 \pm 10^{+13}_{-12}$ GeV, obtained when they assume that their observed excess of top-like events is due to top production. This supports the prediction of the Standard Model that the bulk of weak radiative corrections to electroweak observables is indeed due to the top quark.

Detailed studies of the theoretical uncertainties in the Standard Model predictions are carried out in the working group on 'Precision Calculations at LEP-I' [64]. The theoretical uncertainties are dominated by the uncertainty in the value of $\alpha(m_{\rm Z}^2)$ due to the contribution of light quarks to the photon vacuum-polarisation. For the results presented in this section, a value of $1/\alpha(m_{\rm Z}^2) = 128.79 \pm 0.12$ [66] is used, where the error is propagated in the fits. This uncertainty causes an error of 0.0003 on $\sin^2\theta^{\rm lept}_{\rm eff}$ and 6 GeV on $m_{\rm t}$.

The measurement of $R_{\rm b}$ causes the largest χ^2 contribution of all LEP data in the Standard Model

	Measurement	Standard Model Fit	Pull
a) LEP			
line-shape and lepton asymmetries:			
$m_{\rm Z}$ [GeV]	91.1888 ± 0.0044	91.1887	0.0
$\Gamma_{\rm Z}$ [GeV]	2.4974 ± 0.0038	2.4973	0.0
$\sigma_{\rm h}^0$ [nb]	41.49 ± 0.12	41.437	0.4
R_ℓ	20.795 ± 0.040	20.786	0.2
$A_{\rm FB}^{0,\,\ell}$	0.0170 ± 0.0016	0.0153	1.0
+ correlation matrix Table 8			
τ polarisation:			
$\mathcal{A}_\tau$	0.143 ± 0.010	0.143	0.0
$\mathcal{A}_{\rm e}$	0.135 ± 0.011	0.143	-0.7
b and c quark results:			
$R_{\rm b}$	0.2202 ± 0.0020	0.2158	2.2
$R_{\rm c}$	0.1583 ± 0.0098	0.172	-1.4
$A_{\rm FB}^{0,\,\rm b}$	0.0967 ± 0.0038	0.1002	-0.9
$A_{\rm FB}^{0,\,\rm c}$	0.0760 ± 0.0091	0.0714	0.5
+ correlation matrix Table 15			
$\rm q\overline{q}$ charge asymmetry:			
$\sin^2\theta_{\rm eff}^{\rm lept}$ ($\langle Q_{\rm FB}\rangle$)	0.2320 ± 0.0016	0.2320	0.0
b) $\rm p\overline{p}$ and νN			
$m_{\rm W}$ [GeV] ($\rm p\overline{p}$ [62])	80.23 ± 0.18	80.32	-0.5
$1 - m_{\rm W}^2/m_{\rm Z}^2$ (νN [7–9])	0.2253 ± 0.0047	0.2242	0.2
c) SLC			
$\sin^2\theta_{\rm eff}^{\rm lept}$ ($A_{\rm LR}$ [6])	0.2294 ± 0.0010	0.2320	-2.6

Table 18: Summary of measurements included in the combined analysis of Standard Model parameters. Section a) summarises LEP averages, section b) electroweak precision tests from $\rm p\overline{p}$ colliders and νN-scattering, section c) gives the result for $\sin^2\theta_{\rm eff}^{\rm lept}$ from the measurement of the left-right polarisation asymmetry at SLD. The Standard Model fit results in column 3 and the pulls (difference to measurement in units of the measurement error) in column 4 are derived from the fit including all data (Table 19, column 4) for a fixed value of $m_{\rm H} = 300$ GeV.

fits presented above (see also Table 18). There is a strong correlation (of -0.4) between the $R_{\rm b}$ and $R_{\rm c}$ measurements; the agreement between $R_{\rm b}$ and its Standard Model prediction improves from 2.2 to 1.9 standard deviations if the value of $R_{\rm c}$ is fixed to the Standard Model value $R_{\rm c} = 0.171$. In this case one obtains $R_{\rm b} = 0.2192 \pm 0.0018$.

Attributing the deviation of $R_{\rm b}$ to the b partial width, R_ℓ should also be affected since $\Gamma_{\rm b\bar{b}}$ is a component of the total hadronic width [67]. In Figure 5 the measured value of $R_{\rm b}$ is plotted versus $\sin^2\theta_{\rm eff}^{\rm lept}$. If one assumes the Standard Model dependence on $\sin^2\theta_{\rm eff}^{\rm lept}$ for the light quark widths and taking $\alpha_s(m_{\rm Z}^2) = 0.123 \pm 0.006$, R_ℓ imposes a constraint on the two variables. The one-sigma R_ℓ band

	LEP	LEP + $p\overline{p}$ and νN data	LEP + $p\overline{p}$ and νN data + A_{LR} from SLD
m_t (GeV)	$173^{+12\ +18}_{-13\ -20}$	$171^{+11\ +18}_{-12\ -19}$	$178^{+11\ +18}_{-11\ -19}$
$\alpha_s(m_Z^2)$	$0.126 \pm 0.005\ \pm 0.002$	$0.126 \pm 0.005\ \pm 0.002$	$0.125 \pm 0.005\ \pm 0.002$
χ^2/d.o.f.	7.6/9	7.7/11	15/12
$\sin^2\theta_{eff}^{lept}$	$0.2322 \pm 0.0004\ ^{+0.0001}_{-0.0002}$	$0.2323 \pm 0.0003\ ^{+0.0001}_{-0.0002}$	$0.2320 \pm 0.0003\ ^{+0.0000}_{-0.0002}$
$1 - m_W^2/m_Z^2$	$0.2249 \pm 0.0013\ ^{+0.0003}_{-0.0002}$	$0.2250 \pm 0.0013\ ^{+0.0003}_{-0.0002}$	$0.2242 \pm 0.0012\ ^{+0.0003}_{-0.0002}$
m_W (GeV)	$80.28 \pm 0.07\ ^{+0.01}_{-0.02}$	$80.27 \pm 0.06\ ^{+0.01}_{-0.01}$	$80.32 \pm 0.06\ ^{+0.01}_{-0.01}$

Table 19: Results of fits to LEP and other electroweak precision data for m_t and $\alpha_s(m_Z^2)$. No external constraint on $\alpha_s(m_Z^2)$ has been imposed. The second column presents the results obtained using LEP data only (Table 18a). In the third column also the combined data from the $p\overline{p}$ collider and νN experiments (Table 18b) are included. The fourth column gives the result when the SLD measurement of the left-right asymmetry (Table 18c) is also added. The central values and the first errors quoted refer to $m_H = 300$ GeV. The second errors correspond to the variation of the central value when varying m_H in the interval $60 \leq m_H\ [\mathrm{GeV}] \leq 1000$. The bottom part of the table lists derived results for $\sin^2\theta_{eff}^{lept}$, $1 - m_W^2/m_Z^2$ and m_W.

is centred on the Standard Model prediction while the R_b band is slightly off-set. However, if the value of $\alpha_s(m_Z^2)$ were lower, then the R_ℓ band would move up, increasing the overlap with the R_b and $\sin^2\theta_{eff}^{lept}$ bands.

Figure 6 shows the χ^2 value for the Standard Model fits discussed in Table 19 column 4, as a function of m_t for the three values of m_H (60, 300 and 1000 GeV) considered. It can be seen that the minima of these curves occur at different values of χ^2. This suggests the possibility of extracting constraints on the value of m_H.

The main m_H dependence of the Standard Model predictions for the measurements listed in Table 18 is given by corrections proportional to $\log(m_H)$. The effects of m_H and m_t, however, are correlated for most observables, which weakens the determination of m_H without a direct measurement of m_t. Figure 7 shows the observed value of $\Delta\chi^2 \equiv \chi^2 - \chi^2_{min}$ as a function of m_H, when the CDF value of m_t is used as an additional constraint in the fit. The observed $\Delta\chi^2$ curve exhibits a minimum for low values of m_H. However, the entire range of m_H up to 1000 GeV is accommodated within an interval in $\Delta\chi^2$ of about four, approximately corresponding to a 95% probability range.

Acknowledgements

We would like to thank the SL Division of CERN for the efficient operation of the LEP accelerator, the precise information on the absolute energy scale and their close cooperation with the four experiments. We would also like to thank Z. Wąs for his help in the understanding of radiative effects in hadronic tau decays.

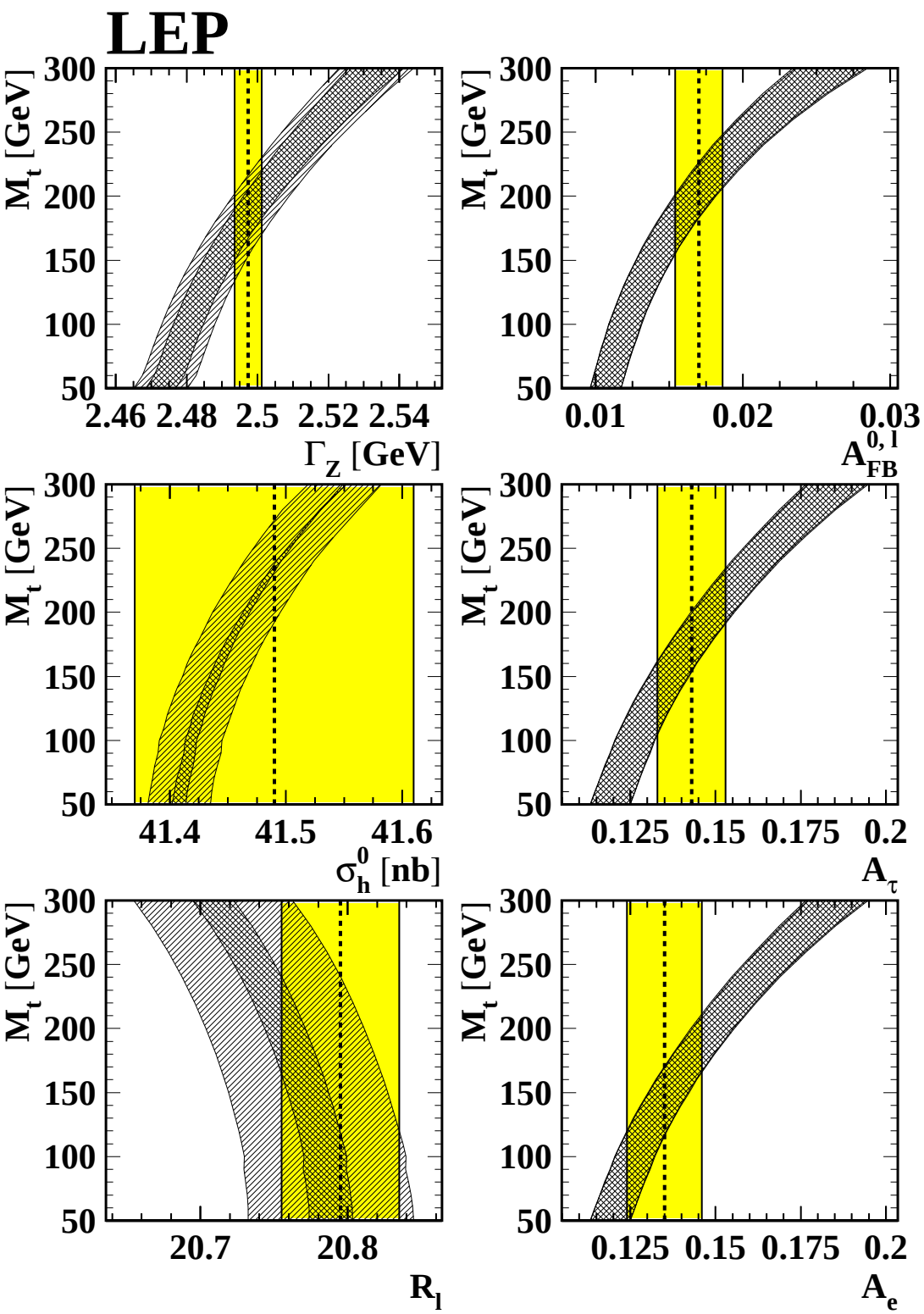

Figure 3: Comparison of LEP measurements with the Standard Model prediction as a function of m_t. The cross-hatched area shows the variation of the Standard Model prediction with m_H spanning the interval $60 < m_H\,(\mathrm{GeV}) < 1000$ and the singly-hatched area corresponds to a variation of $\alpha_s(m_Z^2)$ within the interval $\alpha_s(m_Z^2) = 0.123 \pm 0.006$. The total width of the band corresponds to the linear sum of both uncertainties. The experimental errors on the parameters are indicated as vertical bands.

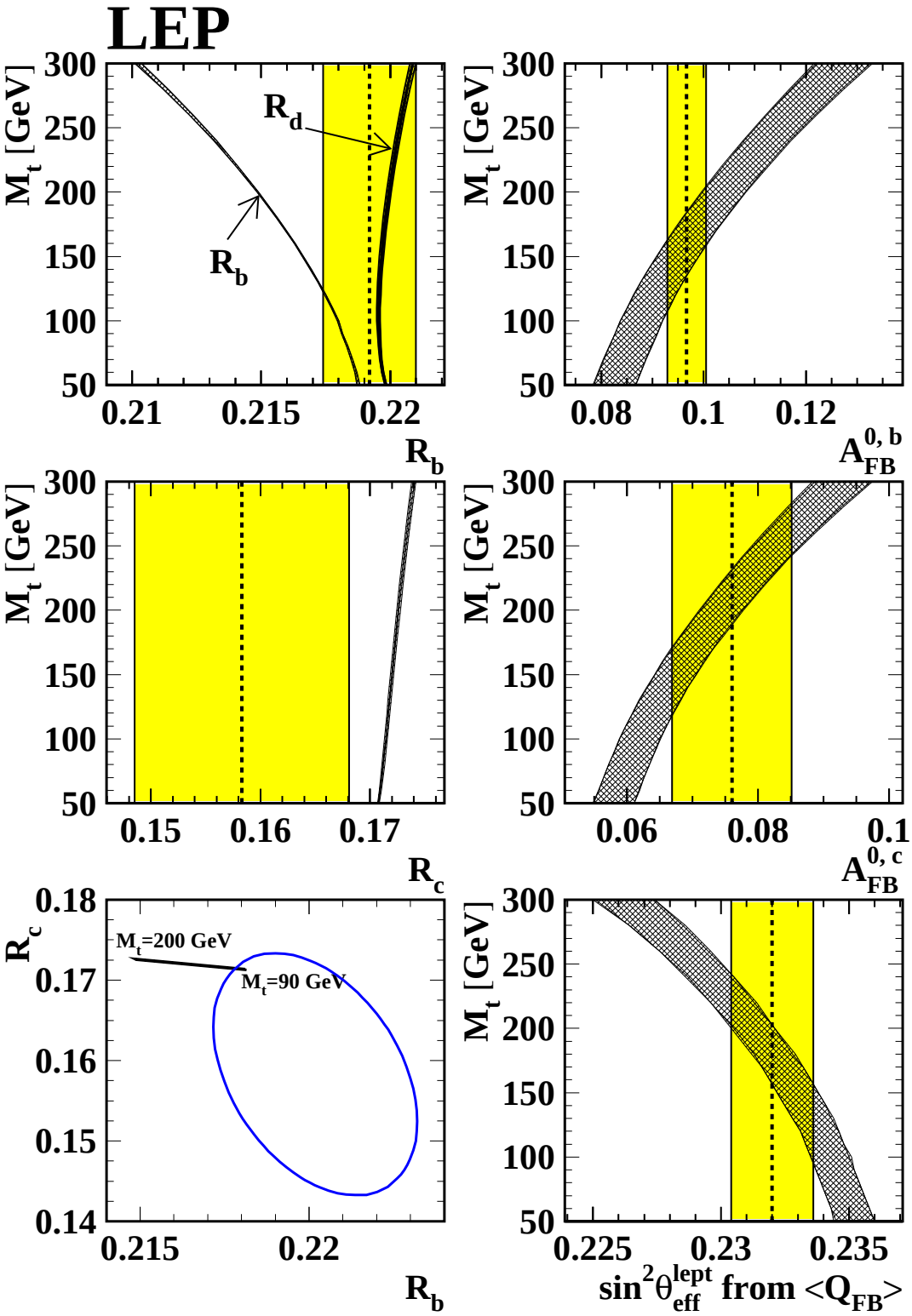

Figure 4: Comparison of LEP measurements with the Standard Model prediction as a function of m_t (*c.f.* figure 3). For ratios of hadronic partial widths this variation with m_H and $\alpha_s(m_Z^2)$ nearly cancels. For the comparison of R_b with the Standard Model the value of R_c has been fixed to the Standard Model. Also shown is the 68% confidence level contour in the R_b-R_c plane together with the Standard Model prediction. To illustrate the impact of special vertex corrections to R_b the Standard Model prediction of R_d is also indicated.

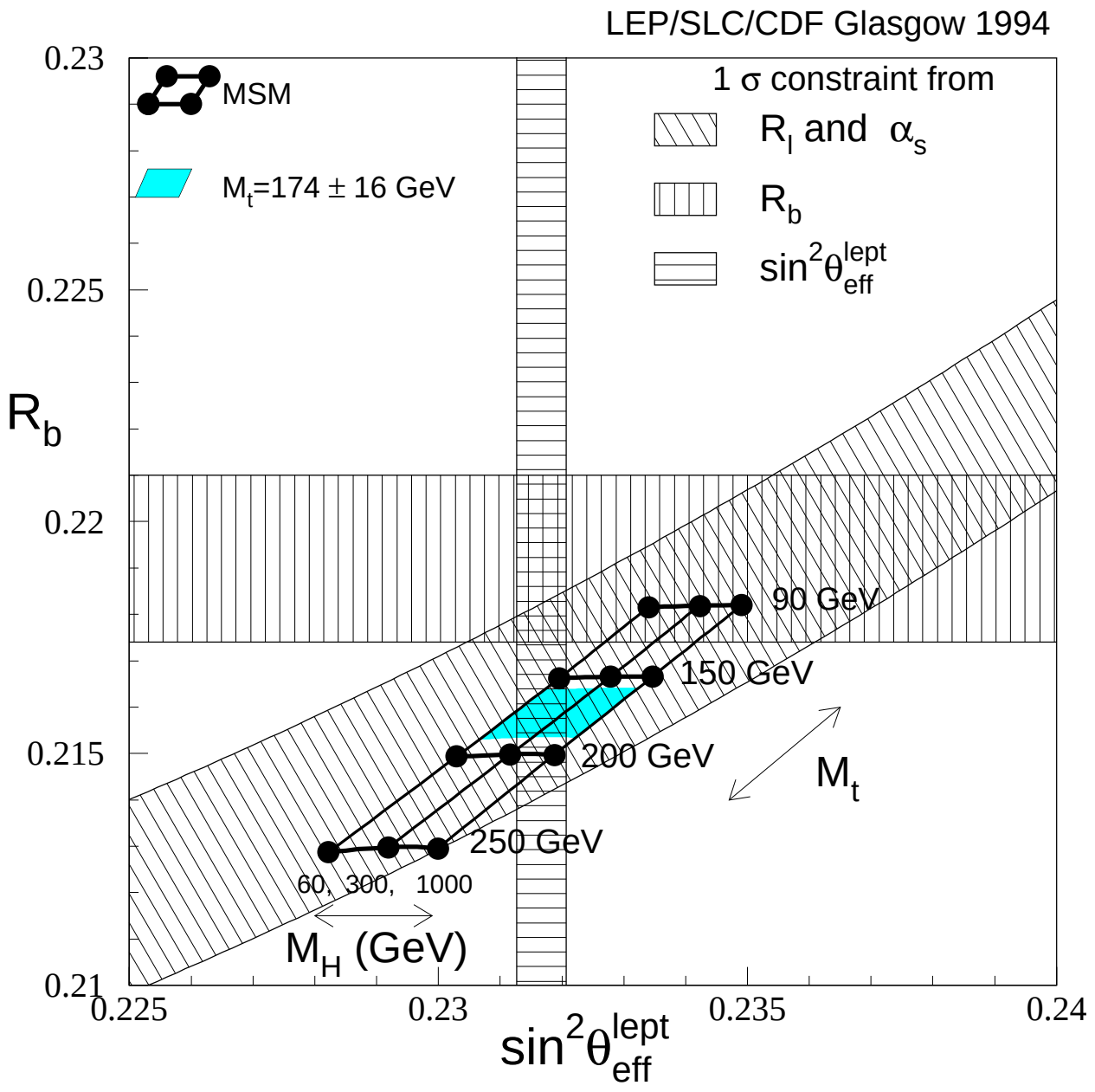

Figure 5: The LEP/SLD measurements of $\sin^2\theta^{\rm lept}_{\rm eff}$ and $R_{\rm b}$ and the Standard Model prediction. Also shown is the constraint resulting from the measurement of R_ℓ on these variables, assuming $\alpha_s(m_{\rm Z}^2) = 0.123 \pm 0.006$, as well as the Standard Model dependence of light quark partial widths on $\sin^2\theta^{\rm lept}_{\rm eff}$.

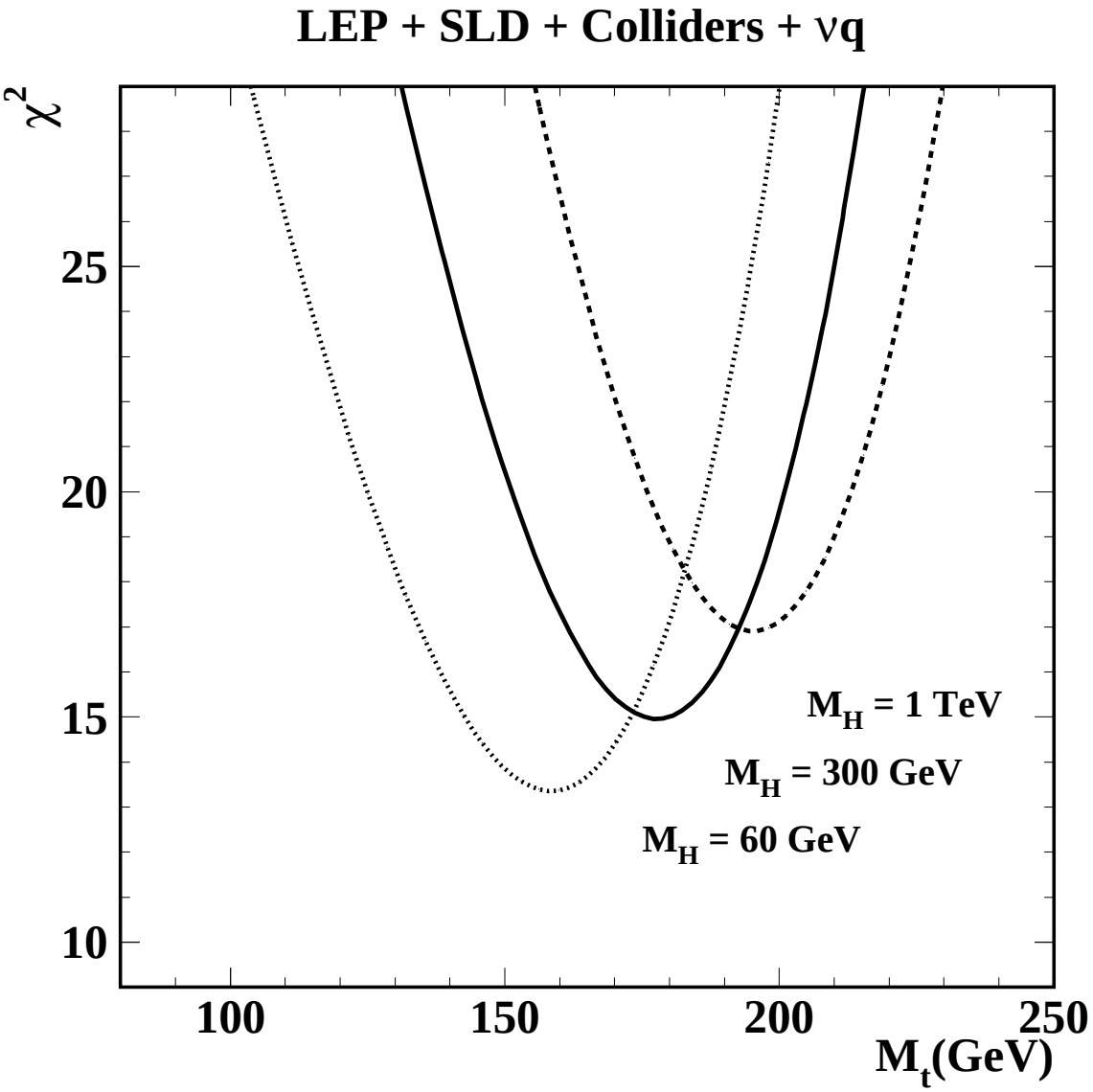

Figure 6: The χ^2 curves for the Standard Model fit in Table 19, column 4 to the electroweak precision measurements listed in Table 18 as a function of $m_{\rm t}$ for three different Higgs mass values spanning the interval $60 \leq m_{\rm H}\,[\mathrm{GeV}] \leq 1000$.

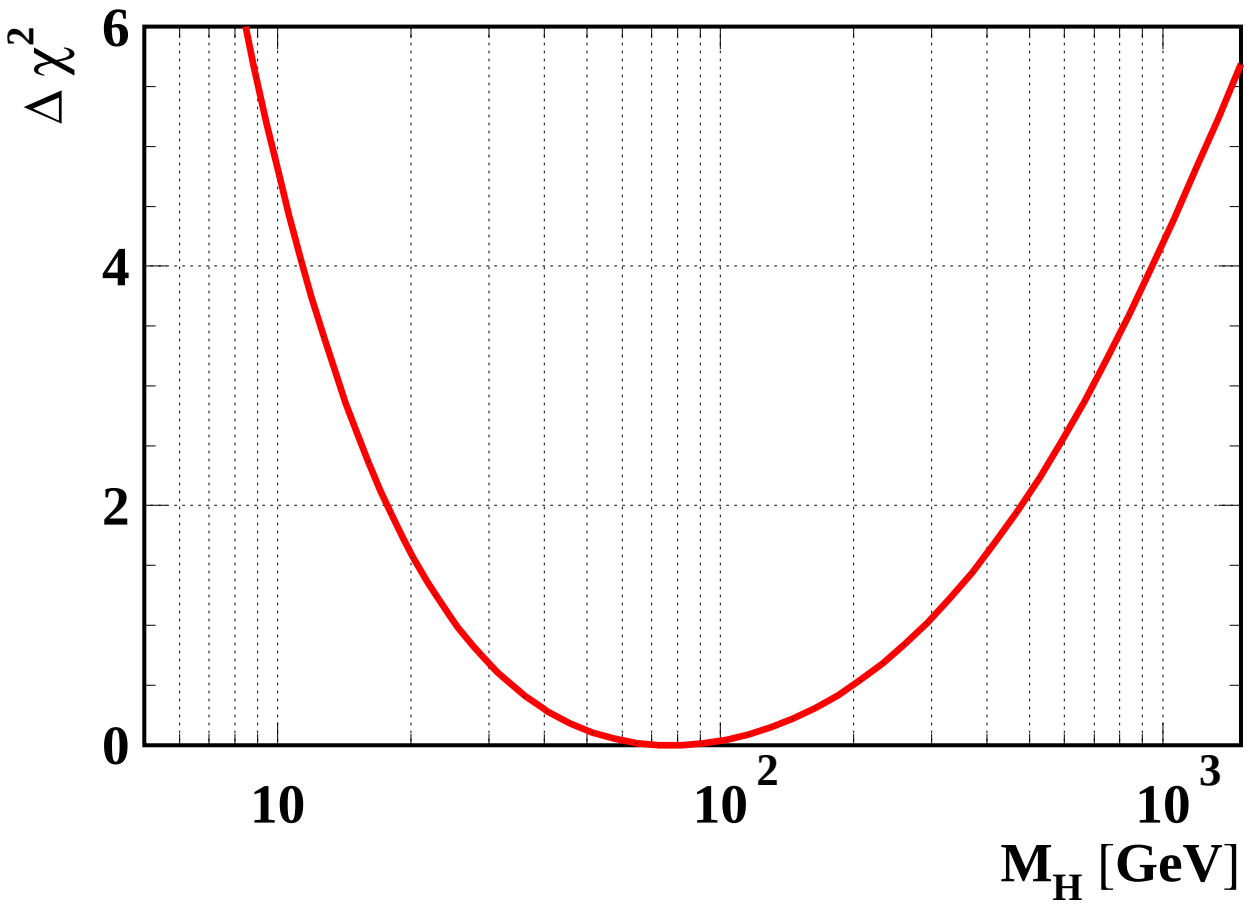

Figure 7: $\Delta\chi^2 = \chi^2 - \chi^2_{min}$ vs $m_{\rm H}$ for the data used in the last column of Table 19 and including the CDF value of $m_{\rm t}$.

Appendix

A The Measurements used in the Heavy Flavour Averages

Tagging	ALEPH 90-91 shape [35]	ALEPH 90-91 lepton [30]	ALEPH 92 lifetime [37]	DELPHI 90-92† multiple [33]	DELPHI 91-92† lepton [39]
R_b	0.2280	0.2162	0.2187	0.2214	0.2145
Statistics	0.0054	0.0062	0.0022	0.0020	0.0089
Uncorrelated	0.0040	0.0033	0.0022	0.0020	0.0063
Correlated	0.0027	0.0038	0.0012	0.0019	0.0023
Total Syst.	0.0048	0.0050	0.0025	0.0028	0.0067
a_c	-0.004		-0.014	-0.018	
R_c^{used}	0.165		0.171	0.171	

Tagging	L3 91 shape [36]	L3 90-91† lepton [31]	OPAL 92-93 multiple [38]	OPAL 90-91 lepton [32]
R_b	0.2220	0.2187	0.2171	0.2252
Statistics	0.0030	0.0081	0.0021	0.0110
Uncorrelated	0.0054	0.0070	0.0011	0.0035
Correlated	0.0036	0.0034	0.0018	0.0057
Total Syst.	0.0065	0.0078	0.0021	0.0066
a_c	-0.021	-0.023	-0.019	-0.014
R_c^{used}	0.171	0.171	0.171	0.171

Table 20: The measurements of R_b. Preliminary results are indicated by the symbol †. The correlated systematic entries are from sources shared with one or more other results in the table; the uncorrelated systematic entries are from the remaining sources. a_c denotes the dependence on the assumed R_c^{used}, which is also given. There is an additional +0.2 statistical and +0.2 systematic correlation between the first two ALEPH results [30, 35].

Tagging	ALEPH 90-91 lepton [30]	DELPHI 91-92† D [42]	DELPHI 91-92† lepton [39]	OPAL 90-92 $D^{*\pm}$ [43]
R_c	0.1670	0.2090	0.1625	0.1410
Statistics	0.0054	0.0190	0.0085	0.0080
Uncorrelated	0.0149	0.0257	0.0177	0.0143
Correlated	0.0114	0.0000	0.0110	0.0000
Total Syst.	0.0188	0.0257	0.0209	0.0143

Table 21: The measurements of R_c.

Tagging	ALEPH 90-93† lepton [30]	ALEPH 90-93† lepton [30]	ALEPH 90-93† lepton [30]	DELPHI 91-93† lepton [34]	L3 90-93† lepton [31]	OPAL 90-93† lepton [32]	OPAL 90-93† $D^{*\pm}$ [46]
$\sqrt{s}$ (GeV)	88.36	89.42	90.21	89.43	89.56	89.54	89.54
$A_{FB}^{b\bar{b}}(-2)$	-3.1	3.3	9.3	6.3	7.0	3.7	24.0
Statistics	11.0	3.0	5.8	3.8	3.5	3.0	27.0
Uncorrelated	0.0	0.0	0.0	0.2	0.4	0.4	4.6
Correlated	0.1	0.1	0.3	0.2	0.1	0.2	0.9
Total Syst.	0.1	0.1	0.3	0.2	0.4	0.5	4.7

Table 22: The measurements of $A_{FB}^{b\bar{b}}(-2)$ (in units of 10^{-2}).

Tagging	ALEPH 90-93† lepton [30]	ALEPH 91-93 jet [40]	DELPHI 92† jet [34]	DELPHI 91-93† lepton [34]	DELPHI 91-92† $D^{*\pm}$ [45]	L3 90-93† lepton [31]	OPAL 91-92† jet [41]	OPAL 90-93† lepton [32]	OPAL 90-93† $D^{*\pm}$ [46]
$\sqrt{s}$ (GeV)	91.26	91.19	91.28	91.26	91.27	91.27	91.28	91.26	91.26
A_{FB}^{bb}(pk)	8.43	9.92	11.50	10.65	4.60	10.28	9.50	8.72	4.20
Statistics	0.68	0.85	1.80	1.10	5.90	1.00	1.10	1.00	7.90
Uncorrelated	0.08	0.25	0.59	0.33	2.09	0.36	0.30	0.21	2.45
Correlated	0.12	0.28	0.31	0.26	1.22	0.14	0.30	0.23	0.65
Total Syst.	0.14	0.38	0.67	0.42	2.42	0.39	0.42	0.32	2.53

Table 23: The measurements of $A_{FB}^{b\bar{b}}$(pk) (in units of 10^{-2}).

Tagging	ALEPH 90-93† lepton [30]	ALEPH 90-93† lepton [30]	ALEPH 90-93† lepton [30]	DELPHI 91-93† lepton [34]	L3 90-93† lepton [31]	OPAL 90-93† lepton [32]	OPAL 90-93† $D^{*\pm}$ [46]
$\sqrt{s}$ (GeV)	92.07	93.02	93.93	93.02	92.93	92.94	92.94
$A_{FB}^{b\bar{b}}(+2)$	5.1	10.5	11.8	14.9	11.0	11.1	-41.0
Statistics	4.9	2.4	7.5	3.6	2.9	2.6	23.0
Uncorrelated	0.0	0.0	0.0	0.5	0.4	0.4	7.2
Correlated	0.2	0.3	0.3	0.4	0.1	0.4	2.5
Total Syst.	0.2	0.3	0.3	0.6	0.4	0.6	7.6

Table 24: The measurements of $A_{FB}^{b\bar{b}}(+2)$ (in units of 10^{-2}).

Tagging	ALEPH 90-93† lepton [30]	ALEPH 89-91 $D^{*\pm}$ [44]	DELPHI 91-92† lepton [34]	DELPHI 91-92† $D^{*\pm}$ [45]	L3 90-91 lepton [31]	OPAL 90-93† lepton [32]	OPAL 90-93† $D^{*\pm}$ [46]
$\sqrt{s}$ (GeV)	91.26	91.25	91.27	91.27	91.24	91.26	91.26
$A_{FB}^{c\bar{c}}$(pk)	9.10	7.12	8.02	8.10	7.84	4.30	11.00
Statistics	2.00	2.11	2.20	2.90	3.70	1.30	3.70
Uncorrelated	1.54	0.69	1.25	1.14	2.40	0.55	0.97
Correlated	1.04	0.20	0.86	0.34	0.79	0.68	0.73
Total Syst.	1.86	0.72	1.52	1.19	2.53	0.87	1.22

Table 25: The measurements of $A_{FB}^{c\bar{c}}$(pk) from $D^{\star}$ meson and lepton tag analyses (in units of 10^{-2}).

Tagging	OPAL 90-93† lepton [32]	OPAL 90-93† $D^{*\pm}$ [46]	OPAL 90-93† lepton [32]	OPAL 90-93† $D^{*\pm}$ [46]
$\sqrt{s}$ (GeV)	89.54	89.54	92.94	92.94
$A_{FB}^{c\bar{c}}$	-17.8	-7.0	7.6	32.0
Statistics	4.5	12.0	3.8	11.0
Uncorrelated	1.9	1.4	1.3	2.4
Correlated	0.4	0.5	0.2	1.6
Total Syst.	1.9	1.4	1.3	2.9

Table 26: The measurements of $A_{FB}^{c\bar{c}}(-2)$ and $A_{FB}^{c\bar{c}}(+2)$ (in units of 10^{-2}).

Tagging	ALEPH 90-93† lepton [30]	DELPHI 91-92† lepton [39]	L3 90-93† lepton [31]	OPAL 90-93† lepton [32]
BR($b \to \ell$)(%)	11.20	11.21	11.44	10.53
Statistics	0.33	0.45	0.48	0.60
Uncorrelated	0.33	0.50	0.38	0.39
Correlated	0.26	0.48	0.23	0.54
Total Syst.	0.42	0.70	0.43	0.66

Table 27: The measurements of BR($b \to \ell$) from the lepton tag analyses.

Tagging	ALEPH 90-93† lepton [30]	DELPHI 91-92† lepton [39]	OPAL 90-93† lepton [32]
BR($b \to c \to \ell^+$) (%)	8.81	7.70	8.25
Statistics	0.25	0.49	0.40
Uncorrelated	0.40	0.95	0.57
Correlated	0.69	0.83	0.39
Total Syst.	0.80	1.26	0.69

Table 28: The measurements of BR($b \to c \to \ell^+$) from the lepton tag analyses.

Tagging	ALEPH 90-93† lepton [30]	DELPHI 91-92† lepton [39]	L3 90-93† lepton [31]	OPAL 90-93† lepton [32]
$\overline{\chi}$	0.0993	0.1500	0.1253	0.1436
Statistics	0.0073	0.0200	0.0110	0.0220
Uncorrelated	0.0028	0.0107	0.0053	0.0055
Correlated	0.0075	0.0119	0.0062	0.0028
Total Syst.	0.0081	0.0160	0.0081	0.0062

Table 29: The measurements of $\overline{\chi}$ from the lepton tag analyses.

References

[1] The LEP Collaborations, Phys. Lett. **B276** (1992) 247.

[2] The LEP Collaborations ALEPH, DELPHI, L3, OPAL and the LEP Electroweak Working Group, *Updated Parameters of the* Z *Resonance from Combined Preliminary Data of the LEP Experiments*, CERN-PPE/93-157.

[3] LEP Energy Working Group, L. Arnaudon *et al.*, *The Energy Calibration of LEP in 1991*, CERN-PPE/92-125 (1992) and CERN-SL/92-37(DI);
LEP Energy Working Group, ALEPH, DELPHI, L3 and OPAL Collaborations, L. Arnaudon *et al.*, Phys. Lett. **B307** (1993) 187;
LEP Energy Working Group, L. Arnaudon *et al.*, *The Energy Calibration of LEP in 1992*, CERN SL/93-21 (DI), April 1993;
LEP Energy Working Group, L. Arnaudon *et al.*, *Accurate determination of the LEP beam Energy by resonant depolarization*, CERN-SL/94-71 (BI), August 1994.

[4] LEP Energy Working Group, private communication;
M. Koratzinos, Proceedings of the conference: *Results and perspectives in Particle Physics*, La Thuile, March 6-12, 1994.

[5] S. Jadach, E. Richter-Wąs, Z. Wąs and B.F.L. Ward, Phys. Lett. **B268** (1991) 253; Comput. Phys. Commun. **70** (1992) 305;
W. Beenakker and B. Pietrzyk, Phys. Lett. **B304** (1993) 366.

[6] SLD Collaboration, K. Abe *et al.*, Phys. Rev. Lett **73** (1994) 25.

[7] CDHS Collaboration, H. Abramowicz *et al.*, Phys. Rev. Lett. **57** (1986) 298;
CDHS Collaboration, A. Blondel *et al.*, Z.Phys. **C45** (1990) 361.

[8] CHARM Collaboration, J.V. Allaby *et al.*, Phys. Lett. **B177** (1986) 446;
CHARM Collaboration, J.V. Allaby *et al.*, Z. Phys.**C36** (1987) 611.

[9] CCFR Collaboration, C.G. Arroyo *et al.*, Phys. Rev. Lett. **72** (1994) 3452.

[10] UA2 Collaboration, J. Alitti *et al.*, Phys. Lett. **B276** (1992) 354.

[11] CDF Collaboration, F. Abe *et al.*, Phys. Rev. **D43** (1991) 2070.

[12] CDF and D0 preliminary results, Y. Ducros, Proc. of the conference: *Results and Perspectives in Particle Physics*, La Thuile, March 6-12, 1994.

[13] CDF Collaboration, F. Abe *et al.*, Phys. Rev. Lett. **73** (1994) 225.

[14] ALEPH Collaboration, D. Buskulic *et al.*, Z. Phys. **C60** (1993) 71;
ALEPH Collaboration, D. Buskulic *et al.*, Z. Phys. **C62** (1994) 539;
ALEPH Collaboration, *Preliminary Results on Z Production Cross Sections and Lepton Forward-Backward Asymmetries using the 1993 Data*, Contribution to the 27th International Conference on High Energy Physics, Glasgow, Scotland, 20-27 July 1994, ICHEP94 Ref. GLS-0557,GLS-0558.

[15] DELPHI Collaboration, P. Aarnio *et al.*, Nucl. Phys. **B367** (1991) 511;
DELPHI Collaboration, P. Abreu *et al.*, Nucl. Phys. **B417** (1994) 3;
DELPHI Collaboration, P. Abreu *et al.*, Nucl. Phys. B**418** (1994) 403;
DELPHI Collaboration, *Precision Determination of the* Z *Resonance Parameters*, DELPHI 94-102 PHYS 419, July 1994.

[16] L3 Collaboration, B. Adeva *et al.*, Z. Phys. **C51** (1991) 179;
L3 Collaboration, O. Adriani *et al.*, Phys. Rep. **236** (1993) 1;
L3 Collaboration, M. Acciarri *et al.*, Z. Phys. **C62** (1994) 551;
L3 Collaboration, *Results on Electroweak Parameters from L3*, July 1994, L3 Note 1620.

[17] OPAL Collaboration, G. Alexander *et al.*, Z. Phys. **C52** (1991) 175;
OPAL Collaboration, P.D. Acton *et al.*, Z. Phys. **C58** (1993) 219;
OPAL Collaboration, R. Akers *et al.*, Z. Phys. **C61** (1994) 19;
OPAL Collaboration, *A Preliminary Update of the* Z *Line Shape and Lepton Asymmetry Measurements with the 1993 Data*, OPAL Internal Physics Note PN143, July 1994;
OPAL Collaboration, *The Preliminary OPAL SiW luminosity analysis: Results for the 1994 Summer conferences*, OPAL Internal Physics Note PN142, July 1994.

[18] See, for example, M. Consoli *et al.*, in "Z Physics at LEP 1", CERN Report CERN 89-08 (1989), eds G. Altarelli, R. Kleiss and C. Verzegnassi, Vol. 1, p. 7.

[19] The ALEPH and L3 results may be found in J.C.Brient, *Measurement of tau polarization at LEP*, talk given at the 27th ICHEP, Glasgow, Scotland, 20-27 July 1994.

[20] DELPHI Collaboration, *Measurement of the* τ *Polarization in* Z *decays*, DELPHI 94-121 PHYS 438, contributed to the Glasgow Conference.

[21] OPAL Collaboration, R. Akers *et al.*, *Measurement of the Tau Lepton Polarization and its Forward-Backward Asymmetry from* Z *Decays*, CERN-PPE/94-120 (27 July 94), submitted to Z. Phys. C.

[22] S. Jadach, B.F.L. Ward, Z. Wąs, Comp. Phys. Comm. **66** (1991) 276, **79** (1994) 503;
S. Jadach, Z. Wąs, R. Decker, M. Jeżabek, J. H. Kühn, Comp. Phys. Comm. **76** (1993) 361.

[23] E. Barberio, B. van Eijk, Z. Wąs, Comp. Phys. Comm. **66** (1991) 115, CERN-TH 7033/93.

[24] D. Bardin *et al.*, Z. Phys. **C44** (1989) 493; Comp. Phys. Comm. **59** (1990) 303; Nucl. Phys. **B351**(1991) 1; Phys. Lett. **B255** (1991) 290 and CERN-TH 6443/92 (May 1992).

[25] ALEPH Collaboration, D. Buskulic *et al.*, Phys. Lett. B. **321** (1994) 168;
ALEPH Collaboration, *Michel Parameters and* τ *Neutrino Helicity from Spin/Energy Correlations in* $Z \to \tau^+\tau^-$, contributed paper to the Glasgow Conference, ICHEP94 Ref 0573.

[26] ARGUS Collaboration, H. Albrecht *et al.*, Z. Phys C58, (1993) 61;
D. Wegner, *Measurement of the Michel parameters in* τ *decays and the helicity of the* τ *neutrino*, talk given at the 27th ICHEP, Glasgow, Scotland, 20-27 July 1994.

[27] R. Decker and M. Finkemeier, Phys. Rev. **D48** (1993) 4203.

[28] M. Finkemeier, Radiative corrections to the decay $\tau \to \pi\nu$, PhD Thesis, University of Karlsruhe, Feb 1994.

[29] L3 Collaboration, M. Acciarri *et al.*, *A Measurement of* τ *Polarization at LEP*, CERN-PPE/94-145, Sept. 94, to be published in Phys. Lett. B.

[30] ALEPH Collaboration, D. Buskulic *et al.*, Z. Phys. **C62** (1994) 179;
ALEPH Collaboration, $B^0\overline{B^0}$ *mixing and* $b\overline{b}$ *asymmetry from high* p_t *leptons,* ALEPH 94-036, contributed paper to the La Thuile and Moriond Winter conferences, 1994;
ALEPH Collaboration, *Heavy Flavour Lepton Contribution for Summer 1994 Conferences,* ALEPH 94-123 PHYSIC 94-107.

[31] L3 Collaboration, O. Adriani *et al.*, Phys. Lett. **B292** (1992) 454;
L3 Collaboration, M. Acciarri *et al.*, Phys. Lett. **B335** (1994) 542;
L3 Collaboration, *Measurement of* R_b *and BR(*$b \to \ell X$*) from b-quark semi-leptonic decays,* L3 internal note 1449, July 16 1993;
L3 Collaboration, *L3 Results on* $A_{FB}^{b\bar{b}}$, $A_{FB}^{c\bar{c}}$ *and* χ *for the Glasgow Conference,* L3 Note 1624;
L3 Collaboration, *L3 Results on* R_b *and* BR($b \to \ell$) *for the Glasgow Conference,* L3 Note 1625.

[32] OPAL Collaboration, R. Akers *et al.*, Z. Phys. **C60** (1993) 199;
OPAL Collaboration, *The forward-backward asymmetry of* $e^+e^- \to Z \to b\bar{b}$ *and* $e^+e^- \to Z \to c\bar{c}$ *from events tagged by a lepton,* Contribution to the 27th International Conference on High Energy Physics, Glasgow, Scotland, 20-27 July 1994, ICHEP94 Ref. GLS-0505.

[33] DELPHI Collaboration, *DELPHI Results on Electroweak Physics with Quarks*, DELPHI 94-111 PHYS 428, contributed paper to the Glasgow Conference, and references therein.

[34] DELPHI Collaboration, *Measurement of the Forward-Backward asymmetry of* $e^+e^- \to Z \to b\bar{b}$ *using prompt leptons and a microvertex tag,* DELPHI 94-62 PHYS 383.

[35] ALEPH Collaboration, D. Buskulic *et al.*, Phys. Lett. **B313** (1993) 549.

[36] L3 Collaboration, O. Adriani *et al.*, Phys. Lett. **B307** (1993) 237.

[37] ALEPH Collaboration, D. Buskulic *et al.*, Phys. Lett. **B313** (1993) 535.

[38] OPAL Collaboration, *Measurement of* $\Gamma_{b\bar{b}}/\Gamma_{had}$ *using a Double Tagging Method,* CERN-PPE/94-106, submitted to Z. Phys. C.

[39] DELPHI Collaboration, *Measurement of* R_b *using microvertex and lepton double tags,* DELPHI 94-91 PHYS 408.

[40] ALEPH Collaboration, D. Buskulic *et al.*, Phys. Lett. **B335** (1994) 99.

[41] OPAL Collaboration, *A Measurement of the Forward-Backward asymmetry of* $e^+e^- \to b\bar{b}$ *using a jet charge algorithm and lifetime tagged events,* OPAL Internal Physics Note PN127, March 1994.

[42] DELPHI Collaboration, *Study of D, D* and D** Production in Z hadronic decays*, DELPHI 94-103 PHYS 420.

[43] OPAL Collaboration, *A Measurement of the Production of* $D^{*\pm}$ *Mesons on the* Z *Resonance,* Contribution to the 27th International Conference on High Energy Physics, Glasgow, Scotland, 20-27 July 1994, ICHEP94 Ref. GLS-0513.

[44] ALEPH Collaboration, D. Buskulic *et al.*, Z. Phys. **C62** (1994) 1.

[45] DELPHI Collaboration, *Measurement of the Forward-backward asymmetry of charm and bottom quarks at the* Z *pole using* $D^{*\pm}$ *mesons,* DELPHI 94-95 PHYS 412.

[46] OPAL Collaboration, *Updated Measurement of the Forward-Backward Asymmetry of* $e^+e^- \to b\bar{b}$ *and* $e^+e^- \to c\bar{c}$ *on and near the* Z *peak using* $D^{*\pm}$ *mesons,* Contribution to the 27th International Conference on High Energy Physics, Glasgow, Scotland, 20-27 July 1994, ICHEP94 Ref. GLS-0516.

[47] LEP Electroweak Working Group, *A Consistent Treatment of Systematic Errors for LEP Electroweak Heavy Flavour Analyses*, LEPHF/94-01, ALEPH Note 94-30, DELPHI 94-23 Phys 357, L3 Note 1577, OPAL Technical Note TN213.

[48] LEP Electroweak Working Group, *Presentation of LEP Electroweak Heavy Flavour Analyses for Summer 1994 Conferences*, LEPHF/94-02, ALEPH Note 94-90, DELPHI 94-23/add, L3 Note 1613, OPAL Technical Note TN237.

[49] LEP Electroweak Working Group, *LEP Electroweak Heavy Flavour Results for Summer 1994 Conferences*, LEPHF/94-03, ALEPH Note 94-119 PHYSIC 94-103, DELPHI 94-108 PHYS 425, L3 Note 1630, OPAL Technical Note TN242.

[50] ALEPH Collaboration, D. Decamp *et al.*, Phys. Lett. **B244** (1990) 551.

[51] DELPHI Collaboration, P. Abreu *et al.*, Phys. Lett. **B252** (1990) 140;
DELPHI Collaboration, P. Abreu *et al.*, Phys. Lett. **B295** (1992) 383.

[52] L3 Collaboration, B. Adeva *et al.*, Phys. Lett. **B241** (1990) 416;
L3 Collaboration, B. Adeva *et al.*, Phys. Lett. **B252** (1990) 703;
L3 Collaboration, B. Adeva *et al.*, Phys. Lett. **B252** (1990) 713;
L3 Collaboration, B. Adeva *et al.*, Phys. Lett. **B288** (1992) 395.

[53] OPAL Collaboration, P. Acton *et al.*, Phys. Lett. **B276** (1992) 379;
OPAL Collaboration, P. Acton *et al.*, Z. Phys. **C55** (1993) 191;
OPAL Collaboration, P. Acton *et al.*, Z. Phys. **C60** (1993) 19;
OPAL Collaboration, G. Alexander *et al.*, Phys. Lett. **B262** (1991) 341;
OPAL Collaboration, R. Akers *et al.*, Z. Phys. **C60** (1993) 601;
OPAL Collaboration, P. Acton *et al.*, Z. Phys. **C58** (1993) 523;
OPAL Collaboration, P. Acton *et al.*, Z. Phys. **C60** (1993) 579;
OPAL Collaboration, R. Akers *et al.*, Z. Phys. **C61** (1994) 357;
OPAL Collaboration, M.Z. Akrawy *et al.*, Phys. Lett. **B263** (1991) 311.

[54] B. Lampe, *A note on QCD corrections to A_{FB}^b using thrust to determine the b-quark direction*, MPI-Ph/93-74.

[55] G. Altarelli and B. Lampe, Nucl. Phys. **B391** (1993) 3.

[56] CHARM II Collaboration, P. Vilain *et al.*, *Precision Measurements of Electroweak Parameters from the Scattering of Muon Neutrinos on Electrons*, CERN-PPE/94-124.

[57] ALEPH Collaboration, D. Decamp *et al.*, Phys. Lett. **B259** (1991) 377.

[58] ALEPH Collaboration, ALEPH-Note 93-041 PHYSIC 93-032 (1993);
ALEPH Collaboration, ALEPH-Note 93-042 PHYSIC 93-034 (1993);
ALEPH Collaboration, ALEPH-Note 93-044 PHYSIC 93-036 (1993).

[59] DELPHI Collaboration, P. Abreu *et al.*, Phys. Lett. **B277** (1992) 371.

[60] OPAL Collaboration, P. D. Acton *et al.*, Phys. Lett. **B294** (1992) 436.

[61] S. Bethke, Proceedings of the Linear Collider Workshop in Waikoloa/Hawaii, April 1993;
S. Catani, Proc. of the EPS Conference on High Energy Physics, Marseille, July 22-28, 1993, Editions Frontieres, Ed. J. Carr-M. Perrottet, page 771;
S. Banerjee, Proc. of the EPS Conference on High Energy Physics, Marseille, July 22-28, 1993, Editions Frontieres, Ed. J. Carr-M. Perrottet, page 299.

[62] M. Demarteau *et al.*, *Combining W Mass Measurements*, CDF/PHYS/CDF/PUBLIC/2552 and D0 NOTE 2115.

[63] Electroweak libraries:
ZFITTER: see Reference 24;
BHM: G. Burgers, W. Hollik and M. Martinez; M. Consoli, W. Hollik and F. Jegerlehner: Proceedings of the Workshop on Z physics at LEP I, CERN Report 89-08 Vol.I,7 and G. Burgers, F. Jegerlehner, B. Kniehl and J. Kühn: the same proceedings, CERN Report 89-08 Vol.I, 55.
These computer codes have recently been upgraded by including the results of:
B. A. Kniehl and A. Sirlin, DESY 92-102;
S. Fanchiotti, B. A. Kniehl and A. Sirlin, CERN-TH.6449/92;
R. Barbieri *et al.*, Phys. Lett. **B288** (1992) 95;
K. G. Chetyrkin and J. H. Kühn, Phys. Lett. **B248** (1990) 359;
K. G. Chetyrkin, J. H. Kühn and A. Kwiatkowski, Phys. Lett. **B282** (1992) 221;
J. Fleischer, O. V. Tarasov and F. Jegerlehner, Phys. Lett. **B293** (1992) 437.

[64] D.Bardin *et al.*, working group on *Precision Calculations at LEP-I*, proceedings of the 1994 workshop in preparation.

[65] T. Hebbeker, M. Martinez, G. Passarino and G. Quast, Phys. Lett. **B331** (1994) 165.

[66] H. Burkhardt, F. Jegerlehner, G. Penso and C. Verzegnassi, Z. Phys. **C 43** (1989) 497.

[67] A. Blondel and C. Verzegnassi, Phys. Lett. **B311** (1993) 346.